이학박사학위논문

척수 통증과민화에서 중추 transient receptor potential vanilloid-1 수용체의 역할

The role of central transient receptor potential vanilloid-1 receptor in central sensitization of pain in the spinal cord

2012년 8월

서울대학교 대학원

치의과학과 신경생물학 전공

김 용 호

ABSTRACT

The role of central transient receptor potential vanilloid-1 receptor in central sensitization of pain in the spinal cord

Yong Ho Kim

Transient receptor potential vanilloid subtype 1 (TRPV1) is predominantly expressed in central terminals of C-fiber primary sensory neuron and their antagonists have shown efficacy in inflammatory and neuropathic pain. TRPV1 and metabotropic glutamate receptor 5 (mGluR5) located on peripheral sensory terminals have been shown to play critical roles in the transduction and modulation of pain sensation. However, very little is known regarding the significance of functional expression of mGluR5 and TRPV1 on the central terminals of sensory neurons in the dorsal horn of the spinal cord.

In the first chapter, I show that functional coupling of mGluR5-TRPV1 via diacylglycerol (DAG) generated by mGluR5 activation on the central presynaptic terminals of nociceptive neurons may be an important mechanism underlying central sensitization under pathological pain conditions.

A number of recent studies revealed that TRPV1 antagonist attenuated not only thermal hyperalgesia but also mechanical allodynia, which is thought to be independent of peripheral-TRPV1, suggesting that central postsynaptic TRPV1 may be involved in pathological mechanical pain. However, the underlying

mechanisms for the activation of central TRPV1 and role of central postsynaptic TRPV1 under pathophysiological conditions remain unknown.

In the second chapter, I present that activation of spinal TRPV1 induces long-term depression (LTD) in GABAergic substantia gelatinosa (SG) neurons and produces mechanical allodynia by reducing inhibitory inputs to projection neurons. Chronic mechanical pain following nerve injury was reversed by a spinally applied TRPV1 antagonist. Taken together, spinal TRPV1 plays a critical role as a synaptic regulator and suggest the utility of CNS-specific TRPV1 antagonists for treating neuropathic pain.

CONTENTS

LIST OF FIGURES

Chapter 1

Chapter 2

BACKGROUND

1. Transient receptor potential vanilloid 1 (TRPV1)

The transient receptor potential cation channel subfamily V member 1 (TRPV1), also known as the capsaicin receptor and the vanilloid receptor 1, was initially tested using capsaicin without their molecular identities in peripheral neuron. Capsaicin induced currents were first reported by Bevan and Szolcsanyi (Bevan and Szolcsanyi, 1990). Capsaicin induces inward currents in a dose dependent manner and reverses at a membrane potential of 0 mV, suggesting that capsaicin activates a nonselective cation channel (Bevan and Szolcsanyi, 1990; Urban and Dray, 1993). Single-channel conductance of capsaicin activated channels was much greater at a membrane potential of $+ 60$ mV than $- 60$ mV and their open probability were increased by membrane depolarization (Oh et al., 1996), suggesting capsaicin induced currents are outwardly rectifying and potentially voltage dependent (Piper et al., 1999; Gunthorpe et al., 2000).

In 1997, the first vanilloid (capsaicin) receptor, TRPV1 was cloned by David Julius and colleagues (Caterina et al., 1997). TRPV1 encoding an 838 amino acid protein (~95 kDa) has putative six transmembrane domains with pore-forming hydrophobic region between the fifth and sixth transmembrane domains and two intracellular cytosolic tails in N- and C-termini with three ankyrin repeats in the N-terminus (Caterina et al., 1997; Szallasi et al., 2007).

2. Mechanisms of TRPV1 activation

TRPV1 is activated not only by vanilloids, such as capsaicin, but also by noxious heat (>43°C) and low pH (Caterina et al., 1997; Tominaga et al., 1998), ethanol (Caterina et al., 1997; Trevisani et al., 2002) and various lipids metabolites including *N*-arachidonoyl-ethanolamine (anandamide), *N*-arachidonoyl-dopamine, *N*-oleoyldopamine, lipoxygenase products, such 12- and 15(*S*)-hydroperoxyeicosatetraenoic acid (12-(*S*)-HPETE and 15-(*S*)-HPETE), 5- and 15-(*S*)-hydroxyeicosatetraenoic acids (5-(*S*)-HETE, 15-(*S*)-HETE) (Zygmunt et al., 1999; Hwang et al., 2000; Kwak et al., 2000; Caterina and Julius, 2001; Huang et al., 2002; Shin et al., 2002; Bhave et al., 2003; Chu et al., 2003).

Intracellular capsaicin binding sites of TRPV1 has been confirmed using a synthetic water-soluble capsaicin analogue DA-5018, which is membrane impermeable (Jung et al., 1999). Several key residues of TRPV1 for binding of capsaicin and other agonists have been identified using comparison of TRPV1 channel response to distinct agonists and their sequence alignment throughout different species (Jordt and Julius, 2002; Correll et al., 2004; Phillips et al., 2004; Ohta et al., 2005; Sutton et al., 2005). Avian TRPV1 ortholog was cloned from chicken DRG which was insensitive to capsaicin but had a normal response to heat and low pH. Multiple sequence analysis revealed that avian TRPV1 and rat TRPV1 have a number of differences in the TM2 and TM4 domains. Using point-mutagenesis of the rat TRPV1, the essential role of Y511 and adjacent S512 for capsaicin response was confirmed, whereas heat- and pH-induced response remained (Jordt and Julius, 2002).

Acidification of the extracellular condition (pH<6.0) can leads to channel

activation probably through different opening mechanism from capsaicin. Extracellular proton elicited TRPV1 channel current when applied to outside-out manner, but not in inside-out manner (Tominaga et al., 1998). Site-directed mutagenesis revealed that Glu 648 in extracellular domain is a crucial site for proton-induced TRPV1 activation. In addition, Glu 600 in extracellular domain has a role of proton-induced potentiation of TRPV1 activity (Jordt et al., 2000), suggesting that protons act on the extracellular domain of TRPV1 for modulation and activation of TRPV1.

Since TRPV1, first thermo-TRP channel, was found, several thermo-TRP ion channels were identified, which include TRPV2, TRPV3, TRPV4, TRPM8 and TRPA1, suggesting that temperature sensor domains are present in these TRP ion channel family proteins (Caterina et al., 1999; Peier et al., 2002a; Peier et al., 2002b; Story et al., 2003; Chung et al., 2004). Although key residues of selective heat-sensing site in thermo-TRP channel have not been found, heat-induced TRPV1 single-channel conductance was observed using inside-out membrane patches demonstrating that TRPV1 is a direct heat sensor (Tominaga et al., 1998). A few potential candidates of heat-sensing domain were suggested that C-terminal cytoplasmic tail and voltage-dependent domain of TRPV1 may be involved in thermo-sensing activity (Vlachova et al., 2003; Voets et al., 2004).

3. TRPV1 in nociception

TRPV1 receptors are strongly expressed in the peripheral nervous system (PNS) including C polymodal nociceptive and Aδ nociceptive primary afferent

terminals (Michael and Priestley, 1999; Guo et al., 2001; Valtschanoff et al., 2001). TRPV1 in primary afferent terminals can detect noxious heat and convey painful signals to avoid potential tissue damage. In physiological condition, TRPV1 deficient mice showed an impaired pain nociception by acute thermal stimuli (Caterina et al., 2000; Davis et al., 2000). In inflammation, increased heat sensitivity was normally observed. Using mice model of inflammation induced by Complete Freund's Adjuvant (CFA) and carrageenan, TRPV1 deficient mice exhibited relatively less thermal hypersensitivity (Caterina et al., 2000; Davis et al., 2000) suggesting that inflammation potentiates TRPV1 activity in nociceptive neurons.

A number of inflammatory mediators involved in TRPV1 sensitization have been reported, which include bradykinin, adenosine 5'-triphosphate (ATP), nerve growth factor (NGF) and prostaglandins (Caterina et al., 2000; Davis et al., 2000; Chuang et al., 2001; Moriyama et al., 2003; Bolcskei et al., 2005; Moriyama et al., 2005). The inflammatory mediators bind to G-protein-coupled receptor (GPCR), which activates PKA- (De Petrocellis et al., 2001; Bhave et al., 2002; Rathee et al., 2002) and PKC-pathways (Premkumar and Ahern, 2000; Sugiura et al., 2002) to phosphorylate TRPV1.

PKA-dependent phosphorylation at Ser 116, Thr 144, Thr 370 and Ser 502 residues of TRPV1 play an important role in the development of hyperalgesia by inhibiting TRPV1 desensitization (Bhave et al., 2002; Mohapatra and Nau, 2003) and sensitizing heat-evoked TRPV1 responses (Rathee et al., 2002). Also, PKC-dependent phosphorylation at Ser 502 and Ser 800 residues of TRPV1 can sensitize TRPV1 activity induced by heat, capsaicin and proton (Numazaki et al., 2002; Bhave et al., 2003). Furthermore, these TRPV1 phosphorylation can

facilitate TRPV1 trafficking to the plasma membrane (Zhang et al., 2005). In addition, NGF induced hyperalgesia by both increasing trafficking level of TRPV1 channels in neuronal membrane (Morenilla-Palao et al., 2004; Zhang et al., 2005) and upregulating the expression level of TRPV1 (Ji et al., 2002; Puntambekar et al., 2005).

4. Substantia gelatinosa (SG) in nociceptive processing

The substantia gelatinosa (SG) of the spinal dorsal horn in lamina II receives central inputs of heavily myelinated Aδ-fibers carrying innocuous mechanical stimuli, lightly myelinated Aδ-fibers and unmyelinated c-fibers carrying noxious, temperature and itch sensations (Woolf and Fitzgerald, 1983; Yoshimura and Jessell, 1989). Interestingly, TRPV1 is predominantly expressed in central terminals of C-fiber primary sensory neuron in lamina I-II of the spinal cord.

The SG is the first synaptic area of nociceptive signaling via projection neurons to higher brain centers. SG neurons have been classified into at least four different types by morphology based on orientation and position of cell soma, dendrites and axons; vertical, radial, islet and central cells (Todd and Spike, 1993; Yasaka et al., 2007). Prominent proportion of the local circuitry in SG is inhibitory connection of GABAergic neurons and glycinergic neurons (Todd and McKenzie, 1989; Todd and Sullivan, 1990). These inhibitory interneurons have been proposed as a gate of pain transmission and other sensory modalities to the higher brain centers (Melzack and Wall, 1965). It has also been proved that inhibition of spinal cord, especially dorsal horn, is very

important to prevent developing hyperalgesia and allodynia (Yaksh, 1989; Sivilotti and Woolf, 1994), indicating that tonic inhibition via GABA receptors and glycine receptors is necessary for maintaining normal sensory responses.

5. Central sensitization of the spinal cord

Central sensitization is an increase in neuronal excitability within the central nervous system, so that innocuous stimuli become perceived as pain (Woolf et al., 1992). The increased neuronal excitability is generated by periperal nociceptors of injured- or inflamed site. Continuous nociceptive inputs from PNS can alter the strength of synaptic efficacy in the spinal circuits via synaptic facilitation or a reduction in inhibition (Woolf and Salter, 2000), leading to increase the gain of nociception and maintaining a chronic pain state (Campbell and Meyer, 2006). The early changes in synaptic connectivity are caused by excessive releasing of transmitters or modulators such as glutamate and neuropeptides, which induces synaptic receptors phosphorylation (Ultenius et al., 2006) and enhances channel trafficking to synapse in the post-synpatic neurons (Iwata et al., 2007). In addition, a loss of GABAergic inhibition in the spinal cord through microglial BDNF induced down-regulation of the potassium chloride cotransporter 2 (KCC2) (Coull et al., 2005) and cell death of spinal inhibitory neurons (Scholz et al., 2005) contributes to pain hypersensitivity.

Recent studies have shown that TRPV1 receptors are also expressed in several regions of the CNS including brain regions such as the hippocampus as well as the spinal dorsal horn (Valtschanoff et al., 2001; Gibson et al., 2008).

Interestingly, TRPV1 immunoreactivity in the spinal dorsal horn is partly due to existence of postsynaptic TRPV1 and neurotransmission in superficial dorsal horn is modulated by TRPV1 agonists after dorsal rhizotomy (Valtschanoff et al., 2001; Zhou et al., 2009). Furthermore, TRPV1-mediated increases in neurotransmitter release from nociceptive primary afferent terminals in spinal cord has been reported (Yang et al., 1998; Sikand and Premkumar, 2007). Thus, TRPV1 activation in both primary afferent terminals and spinal neurons may affect to synaptic transmission of the spinal cord.

Consistently, spinal TRPV1 activation can cause mechanical allodynia via central sensitization (Patwardhan et al., 2009) and spinal administration of TRPV1 antagonists can attenuate both inflammatory and neuropathic mechanical pain (Patapoutian et al., 2009), suggesting that TRPV1 may contribute to pain hypersensitivity under pathological pain conditions (Caterina et al., 2000; Kanai et al., 2006). However, distinct roles and molecular mechanisms for presynaptic and postsynaptic TRPV1 action in pain hypersensitivity remain unknown.

PURPOSE

In this thesis study, I have explored the role of TRPV1 in the spinal cord nociceptive circuitry. Further, I have investigated its contribution to the enhancement of pain sensitivity through presynaptic mechanism in central terminals of nociceptive primary afferent neurons and postsynaptic mechanism in SG neurons of spinal cord. To address these mechanisms, the experiments were performed following specific aims.

- To characterize the mechanism of TRPV1 activation in the spinal cord, especially in nociceptive primary afferent terminal.

- To confirm whether TRPV1 is expressed in spinal cord neurons. If so, what is the role of spinal TRPV1 in these neurons?

- To confirm involvement of TRPV1 in central (spinal) sensitization of pain.

CHAPTER 1:

Membrane-Delimited Coupling of TRPV1 and mGluR5 on Presynaptic Terminals of Nociceptive Neurons

ABSTRACT

Transient receptor potential vanilloid subtype 1 (TRPV1) and metabotropic glutamate receptor 5 (mGluR5) located on peripheral sensory terminals have been shown to play critical roles in the transduction and modulation of pain sensation. To date, however, very little is known regarding the significance of functional expression of mGluR5 and TRPV1 on the central terminals of sensory neurons in the dorsal horn of the spinal cord. Here I show that TRPV1 on central presynaptic terminals is coupled to mGluR5 in a membrane-delimited manner, thereby contributing to the modulation of nociceptive synaptic transmission in the substantia gelatinosa (SG) neurons of the spinal cord. Further, the present results demonstrate that TRPV1 is involved in the pain behaviors induced by spinal mGluR5 activation, and diacylglycerol (DAG) produced by the activation of mGluR5 mediates functional coupling of mGluR5 and TRPV1 on the presynaptic terminals. Thus, mGluR5-TRPV1 coupling on the central presynaptic terminals of nociceptive neurons may be an important mechanism underlying central sensitization under pathological pain conditions.

INTRODUCTION

Peripheral TRPV1 is activated not only by capsaicin, heat, and acid (Caterina et al., 1997; Tominaga et al., 1998; Szallasi and Blumberg, 1999; Clapham, 2003) but also by inflammatory mediator-related molecules including the products of lipoxygenases, anandamide, and other endocannabinoids (Hwang et al., 2000; Julius and Basbaum, 2001; Ralevic et al., 2001; Di Marzo et al., 2002; van der Stelt et al., 2005). Multiple inflammatory mediators have been shown to heighten the sensitivity of nociceptive sensory neurons after binding to their respective G-protein coupled receptors (GPCRs) (Scholz and Woolf, 2002), leading to inflammation-induced thermal hyperalgesia via TRPV1. Group I metabotropic glutamate receptors (especially mGluR5) are expressed together with TRPV1 in dorsal root ganglion (DRG) neurons (Walker et al., 2001a) and are also involved in peripheral sensitization of sensory neurons via G-protein mediated TRPV1 modulation (Huang et al., 2002).

Notably, both mGluR5 and TRPV1 are expressed on the central terminals of primary afferents in the superficial lamina of the spinal dorsal horn, the key site for the transmission of pain sensation (Jia et al., 1999; Valtschanoff et al., 2001). Capsaicin potently increases the frequency, but not the amplitude, of mEPSCs in a DRG-dorsal horn neuronal co-culture system (Sikand and Premkumar, 2007), as well as in a spinal slice condition (Yang et al., 1998), suggesting that TRPV1-mediated neurotransmitter release from presynaptic terminals of nociceptive neurons contributes to nociceptive transmission. Despite these findings, however, the underlying mechanisms for the activation of central presynaptic TRPV1 under pathophysiological conditions remain unknown

16

(Patapoutian et al., 2009).

It is well-known that the modulation of synaptic transmissions in the superficial dorsal horn contributes to the pathophysiology of chronic pain conditions (Woolf and Salter, 2000). Indeed, both spinal mGluR5 and TRPV1 have been demonstrated to contribute to pain hypersensitivity under pathological pain conditions (Caterina et al., 2000; Walker et al., 2001b; Zhu et al., 2005; Kanai et al., 2006). While a functional role for mGluR5 in superficial dorsal horn neurons (i.e. postsynaptic neurons) has recently been demonstrated (Hu et al., 2007), relatively little is known about how presynaptic mGluR5 contributes to nociceptive synaptic transmissions in the spinal dorsal horn.

In the present study, I hypothesized that mGluR5 and TRPV1 are coupled on the central presynaptic terminals of nociceptive neurons, thereby contributing to the pain transmission processing activity exerted by TRPV1. I attempted to elucidate the underlying mechanisms of TRPV1 modulation by mGluR5 activation, as this will likely provide insight into the functional significance of TRPV1 expression in the central nervous system (CNS).

MATERIALS AND METHODS

All surgical and experimental procedures were reviewed and approved by the Institutional Animal Care and Use Committee at the School of Dentistry, Seoul National University.

Behavioral studies

All animals were placed in an observation chamber ($60 \times 100 \times 60$ mm each) and allowed to habituate. A mirror was positioned behind the observation chamber to provide an unobstructed view. Spontaneous pain behaviors were assessed by measuring the time each animal spent flinching, licking and/or biting its hindpaws or tail. The cumulative time spent flinching, licking or biting hindpaws or tails during a 5 min period was recorded immediately prior to drug administration and then again up to 210 min after drug administration. For mechanical sensitivity (von Frey filaments) testing, mice were brought from the animal colony and placed in transparent plastic boxes ($60 \times 100 \times 60$ mm) on a metal mesh floor (3×3 mm mesh). The mice were then left alone for at least 20 min to allow them to acclimate prior to testing. To assess mechanical sensitivities, the withdrawal threshold of the hindpaw was measured using a series of von Frey filaments (0.20, 0.69, 1.57, 3.92, 5.88, 9.80, 19.60 and 39.20 mN, Stoelting, Wood Dale, IL, USA; equivalent in grams to 0.02, 0.07, 0.16, 0.40, 0.60, 1.0, 2.0 and 4.0). The 50% withdrawal threshold was determined using the up-down method as previously described (Chaplan et al., 1994). A brisk hindpaw lift in response to von Frey filament stimulation was regarded as

18

a withdrawal response. The 0.4 g filament was the first stimulus to be used, and, when a withdrawal response was obtained, the next weaker filament was used. This process was repeated until no response was obtained, at which time the next stronger filament was administered. Interpolation of the 50% threshold was then carried out using the method of Dixon (Dixon, 1980). All behavioral testing was performed by an investigator who was blind to the genetic background of the mice.

Intrathecal injection of Drug

(R,S)-3,5-dihydroxyphenylglycine (DHPG) was dissolved in 0.9% saline using an ultrasonic washer and applied intrathecally. The dose used in this study was 15 nmol. Intrathecal administration was performed as described previously (Hylden and Wilcox, 1980). Briefly, under slight enflurane anesthesia (2% in 95% O_2), the vertebral column of mouse was held using the thumb and middle finger of the left hand and the drug was injected intrathecally into each mouse using a 25 μl Hamilton syringe fitted with 31 gauge needle at approximately the lumbar enlargement level of the spinal cord. The injection volume was 5 μl and the injection sites were verified by injecting a similar volume of 1% methylene blue solution and determining the distribution of the injected dye in the spinal cord. Before conducting experiments, the injection method was practiced until the success rate was consistently over 95%.

DRG preparation

DRG neurons obtained from 4- to 7-day-old neonatal rats were prepared as

previously described (Oh et al., 2001). Briefly, animals were decapitated, and DRGs were rapidly removed under aseptic conditions and placed in HBSS (Welgene, Korea). DRGs were digested in 1 mg/ml collagenase A (Roche) and 2.4 unit/ml dispase II (Roche) in HBSS for 10 min respectively, followed by 20 min in 0.125% trypsin (Sigma), all at 37°C. The DRGs were then washed in DMEM (Welgene, Korea) 3 times and resuspended in F12 media supplemented with 10% FBS (Gibco) and 1% penicillin/ streptomycin (Sigma). DRGs were then mechanically dissociated using fire-polished glass pipettes, centrifuged (800 RPM, 5 min), resuspended in F12 media supplemented with 5% FBS (Gibco), 20 ng/ml NGF (Invitrogen), 1X N-2 supplement (Invitrogen) and 1% penicillin/ streptomycin (Gibco), and plated on 0.5 mg/ml poly-L-ornithine (Sigma) coated glass coverslips. Cells were maintained at 37°C in 5% CO_2 incubator.

Cell culture and transient transfection

Human embryonic kidney (HEK)-293 cells (American Type Culture Collection, Manassas, VA) were maintained according to the supplier's recommendations. For transient transfections, cells were seeded in 12-well plates. The next day, the cells were transfected with 1 μg/well of pcDNA expression vectors for TRPV1, TRPV1 mutants, or mGluR5 using the lipofectamine 2000 transfection reagent (Invitrogen) according to the manufacturer's suggested protocol. After 18 - 24 hr, cells were trypsinized and used for experiments.

Ca^{2+} imaging

I performed fura-2 AM-based (Molecular Probes, Eugene, OR, USA) Ca^{2+} imaging experiments as previously described (Park et al., 2006). Briefly, the HEK293 cells and DRG neurons prepared were loaded with fura-2 AM (2 μM) for 40 min at 37°C in a balanced salt solution [BSS; containing (in mM): 140 NaCl, 5 KCl, 2 CaCl$_2$, 1 MgCl$_2$, 10 N-[2-hydroxyethyl]piperazine-N'-[2-ethanesulfonic acid] (HEPES), 10 glucose, adjusted to pH 7.3 with NaOH]. Then the cells were rinsed with BSS and incubated in BSS for an additional 30 min to de-esterify the dye. Cells on slides were placed onto an inverted microscope and illuminated with a 175W xenon arc lamp; excitation wavelengths (340/380nm) were selected by a monochromator wavelength changer. Intracellular calcium concentrations ($[Ca^{2+}]_i$) were measured by digital video microfluorometry with an intensified CCD camera (CasCade, Roper Scientific, Trenton, NJ, USA) coupled to the microscope and a computer with Metafluor software (Universal Imaging Corp., PA, USA). All drugs were applied via bath perfusion at a flow rate of 5 ml/min.

Electrophysiology

Whole-cell patch clamp recordings from DRG neurons and spinal SG neurons were performed at room temperature (23 ± 1°C) in normal Tyrode solution as previously described (Oh et al., 2001; Jung et al., 2006). Whole-cell currents from DRG neurons were recorded from 4- to 7-day-old Sprague–Dawley rats (OrientBio, Korea). Whole-cell currents were recorded using an EPC-10 amplifier and Pulse 8.30 software (both from HEKA, Germany). Patch

21

pipettes were made from borosilicate glass and had resistances of 3 - 5 MΩ when filled with standard intracellular solutions. For whole-cell recordings in DRG neurons, I used an external bath solution (normal Tyrode solution) of the following composition (in mM): 140 NaCl, 5 KCl, 2 CaCl$_2$, 1 MgCl$_2$, 10 glucose, and 10 HEPES, adjusted to pH 7.4 with NaOH. The pipette solution contained (in mM) 126 K-gluconate, 10 NaCl, 1 MgCl$_2$, 10 EGTA, 2 NaATP, 0.1 MgGTP, adjusted to pH 7.3 with KOH, and 295 - 300 mOsm. All drug solutions were applied to cells by local perfusion through a capillary tube (1.1 mm inner diameter) positioned near the cell of interest. The solution flow was driven by gravity (flow rate, 4 - 5 ml/min) and controlled by miniature solenoid valves (The Lee Company, Westbrook, CT). For slice patch clamp recordings, Sprague–Dawley rats of both sexes aged 8 - 12 days were used. Before decapitation, the animals were deeply anesthetized with halothane. The spinal cord was exposed by a dorsal laminectomy and dissected out. The lumbosacral segment of spinal cord was placed into ice-cold artificial cerebrospinal fluid (aCSF) and was attached to agarose block (3% in aCSF). Transverse slices (350 - 400   m thick) of the lumbar spinal cord were obtained (VIBRATOME 1000 Plus) and then transferred in aCSF (in mM): 130 NaCl, 3 KCl, 2.5 CaCl$_2$, 1.5 MgSO$_4$, 1.25 NaH$_2$PO$_4$, 25 NaHCO$_3$, 1.25 Hepes, 10 glucose, 20 sucrose, adjusted to pH 7.3, and 310 - 315 mOsm, equilibrated with 95% O$_2$ and 5% CO$_2$) for recovery period of at least 1 hr and then maintained at room temperature in aCSF. The membrane currents were recorded using an EPC-10 amplifier and Pulse 8.30 software. A single slice was placed in a perfusion chamber (0.5 ml volume) and continuously superfused with extracellular solution (3 ml/min) saturated with 95% O$_2$ and 5% CO$_2$. The recording electrodes were filled with a solution containing (in mM); 126 K-

gluconate, 10 NaCl, 1 MgCl$_2$, 10 EGTA, 2 NaATP, 0.1 MgGTP, adjusted to pH 7.3 with KOH, and 295 - 300 mOsm. Whole-cell patch-clamp recordings were made with thin-walled borosilicate glass unpolished pipettes (5 - 7 MΩ) from visually identified SG neurons in the spinal cord slice by using a fixed-stage microscope (BX50WI, Olympus, Japan) with Nomarski optics and a 40× water-immersion objective. All recordings were performed at a holding potential (V$_h$) of -60 mV. mEPSCs were recorded in the presence of 0.5 μM tetrodotoxin (TTX), 5 μM bicuculline, and 2 μM strychnine to block voltage-dependent Na$^+$ channels and activity-dependent sEPSCs, and synaptic inhibition mediated by GABA$_A$ and glycine receptors, respectively. Four-minute stretches of data were used for mEPSC frequency/amplitude analysis. The amplitude threshold for detection of mEPSC was set above the noise level (5 pA) and events were subsequently verified visually. No attempt was made to group the events by the rise time. The Kolmogorov–Smirnov test was used to assess the effects of the DHPG and capsazepine on amplitude and inter-event interval. For cell-attached patch clamp recordings, the recording pipette (6 - 7 MΩ) contained bath solution containing (in mM); 140 NaCl, 5 KCl, 1 MgCl$_2$, 10 glucose, 2 ethylene glycol tetraacetic acid (EGTA) and 10 HEPES, adjusted to pH 7.4 with NaOH. The recordings were performed at a command potential of +40 mV. Drugs were applied into recording pipette or through bath solution. All data were analyzed using single channel analysis program QuB software.

Constructs

An expression vector for TRPV1 containing the point mutation Y511A was produced using a two step PCR approach based on a TRPV1 construct

generated in our lab (Yang et al., 2003). After mutagenesis, the sequence of the final constructs was confirmed by DNA sequencing. pcDNA3.1(+)/mGluR5 were also generated in our lab following conventional methods.

Single-cell reverse transcription-polymerase chain reaction (RT-PCR)

Single-cell RT-PCR was performed as previously described (Park et al., 2006). Entire single cells were aspirated into a patch pipette using negative pressure under visual control. The inner and outer primers used in present study are listed in Table. Negative controls were obtained from pipettes that did not harvest any cell contents, but were submerged in the bath solution.

Table. DNA primers used for single-cell RT-PCR

Target Gene (Product Length) [a]		Outer Primers	Inner Primers	Genbank No.
β-actin (456 bp, 317 bp)	Forward	CCCAGATCATGTTTGAGACC	AGGCTGTGTTGTCCCTGTAT	NM031144
	Reverse	AGGATTCCATACCCAGGAAG	CAGCTCATAGCTCTTCTCCA	
mGluR1 (200 bp, 145 bp)	Forward	CATCATCATTGCCAAACCTGAG	CAGTGCCTTCACGACCTCTGAT	Y18812
	Reverse	CCTGTCTTCCACCTGGTTCAGA	CCATGACACAGACTTGCCGTTA	
mGluR5 (272 bp, 202 bp)	Forward	CCAAACCGGAGAGAAATGTGC	CGCCTTCACAACCTCTACAGTG	NM017012
	Reverse	TTGATGACCGCCGTTTGGT	AGACAGTCGCTGCCACAAATG	
TRPV1 (520 bp, 330 bp)	Forward	ACCGTCAACAAGATTGCACA	TGACTACCGGTGGTGTTTCA	NM031982.1
	Reverse	TGGTTCCCTAAGCAGACCAC	TGATCCCTGCATAGTGTCCA	

[a] (n , n) indicates product size obtained from outer and inner primers, respectively

Electron Microscopy

Three male Sprague-Dawley rats (weight, 300 - 320 g) were used in this study. Tissue samples were prepared as previously described (Bae et al., 2004). An anti-TRPV1 antibody (SC-12498 (P-19), Lot L1302, Santa Cruz, CA, USA) was used. To verify specificity of the antibody, preabsorption controls with a blocking peptide completely abolished the staining (data not shown).

24

Drugs

DHPG, (*RS*)-2-Chloro-5-hydroxyphenylglycine (CHPG), 5'-iodoresiniferatoxin (IRTX), 6-iodonordihydrocapsaicin, 7-(Hydroxyimino)cyclopropa[b]chromen-1a-carboxylate ethyl ester (CPCCOEt), 2-Methyl-6-(phenylethynyl)pyridine hydrochloride (MPEP), staurosporine, and TTX were purchased from Tocris Bioscience (Ellisville, MO). Capsaicin, capsazepine, thapsigargin, bicuculline, stychinin, bisindolylmaleimide (BIM), 1-Oleoyl-2-acetyl-*sn*-glycerol (OAG), 1,6-bis(Cyclohexyloximinocarbonylamino) hexane (RHC80267), 1-[6-[((17β)-3-Methoxyestra-1,3,5[10]-trien-17-yl)amino]hexyl]-1H-pyrrole-2,5-dione (U73122), and 1-[6-[((17β)-3-Methoxyestra-1,3,5[10]-trien-17-yl)amino]hexyl]-2,5-pyrrolidinedione (U73343) were purchased from Sigma (St. Louis, MO).

Statistical Analysis

Data are expressed as mean ± SEM. For behavioral test, statistical analyses of the data obtained from the drug tests were conducted with One-way repeated measures ANOVA followed by a pairwise comparison of pain behaviors before and after the injection, utilizing Bonferroni *t*-test Method. Student's *t*-test was used for the comparison between the knock-out and wild type mice and $P < 0.05$ was considered statistically significant. For other studies, results were compared using Student's *t*-test and $P < 0.05$ was considered statistically significant.

RESULTS

Coupling of group I mGluRs and TRPV1 on central terminals of sensory neurons contributes to pain behaviors

It has been previously demonstrated that spontaneous pain responses are produced by the activation of spinal group I mGluRs (Fisher and Coderre, 1998; Bhave et al., 2001; Hu et al., 2007). I first investigated whether spinal TRPV1 is associated with the spontaneous pain behavior induced by the activation of spinal group I mGluRs using TRPV1 knock-out and wild-type mice. With the intrathecal injection of the vehicle alone, detectable changes in pain behavior compared with the pre-injection baseline was not observed (Figure 1A), suggesting marginal effects of general anesthetics on the pain behaviors observed in the behavioral study. In agreement with previous reports (Fisher and Coderre, 1998; Bhave et al., 2001; Hu et al., 2007), a single intrathecal injection of 15 nmol (*R,S*)-3,5-dihydroxyphenylglycine (DHPG), a selective group I mGluRs (mGluR1/5) agonist, induced an immediate and robust increase in wild-type mice in the time spent either flinching, licking or biting hindpaws or tails (**$P < 0.001$, *$P < 0.05$ vs. pre-injection baseline, one-way repeated measured ANOVA followed by Bonferroni *t*-test) (Figure 2A). I interpreted these responses as signs of spontaneous pain, which persisted up to 120 min after the injection (Figure 1). TRPV1$^{-/-}$ mice lacked this early manifestation of spontaneous pain behaviors following administration of DHPG (Figure 2A). Indeed, the induction of spontaneous pain behavior was markedly delayed so much so that the display of pain behaviors took 20 min after injection to become statistically significant (*$P < 0.05$ vs. pre-injection baseline, One-way

26

repeated measured ANOVA followed by Bonferroni t-test). Further, spontaneous pain was significantly reduced in TRPV1$^{-/-}$ mice in the first 15 min after injection, compared to the wild type mice (##$P < 0.001$, #$P < 0.05$, vs. the wild type mice, Student's t-test), but did not differ thereafter (Figure 1B and Figure 2A). When I examined mechanical sensitivity of hind paws in response to von Frey filaments following intrathecal DHPG injection, mechanical hypersensitivity was persistent throughout the 3.5 hr observation period in wild type mice, but was maintained for only 2 hr in TRPV1$^{-/-}$ mice (*$P < 0.05$ vs. pre-injection baseline, One-way repeated measure ANOVA followed by Bonferroni t-test) (Figure 2B). In addition, mechanical hypersensitivity in TRPV1$^{-/-}$ mice was lower than that of wild type mice (#$P < 0.05$ vs. wild type mice, Student's t-test). Together, these results demonstrated that spinal TRPV1 is associated with DHPG-induced pain behavior, such as spontaneous pain behaviors and mechanical allodynia.

To determine the mechanisms underlying the interactions between group I mGluR receptors and TRPV1 in the spinal cord, I examined whether DHPG regulates TRPV1 activity in synaptic transmission of the spinal dorsal horn. I measured miniature excitatory postsynaptic current (mEPSC) of substantia gelatinosa (SG) neurons from spinal cord slice by using whole-cell patch clamp recording (Figure 3a). In this approach, DHPG had little effect on the amplitude of mEPSC ($97.52 \pm 0.93\%$, n = 4, $P = 0.14$ and $89.90 \pm 4.04\%$, n = 3, $P = 0.13$) (Figure 3c and 3d); however, the frequency of mEPSC was significantly increased by DHPG ($137.87 \pm 2.10\%$, n = 4, $P < 0.001$ and $152.84 \pm 1.19\%$, n = 3, $P < 0.001$) (Figure 3c and 3d), and this was blocked by 5 μM capsazepine, a TRPV1 competitive antagonist ($102.56 \pm 2.08\%$, n = 4, $P = 0.16$) (Figure 3b and 3c) and 6-iodonordihydrocapsaicin, another structurally different TRPV1

antagonist (101.05 ± 2.07%, n = 3, P = 0.83) (Figure 3d). In addition, as shown previously (Tominaga et al., 1998; Hwang et al., 2004), EM analysis demonstrated that TRPV1 was clearly expressed on the perisynaptic region of the presynaptic terminals of sensory neurons in SG (Figure 4). Therefore, I felt it was reasonable to hypothesize that group I mGluRs and TRPV1 coupled on the presynaptic terminals of primary afferents neurons may regulate neurotransmitter releases, thereby contributing to DHPG-induced pain behaviors.

Group I mGluRs drive DHPG-induced Ca^{2+} entry through TRPV1 channels in sensory neurons

Next, I examined how DHPG modulates TRPV1 on presynaptic nociceptive neurons using fura-2 AM based ratiometric Ca^{2+} imaging. DHPG induced a Ca^{2+} response in subpopulations of DRG neurons, acutely isolated from neonatal rats. TRPV1-expressing nociceptive neurons were identified by their responsiveness to a 10 sec application of 200 nM capsaicin at the end of each experiment. In a subpopulation of capsaicin-sensitive neurons (35.74%, n = 89/249), a 20 sec application of 100 μM DHPG induced a transient increase in $[Ca^{2+}]_i$ that produced little desensitization during repetitive application of DHPG (93.90 ± 5.83%, n = 12, P = 0.31) (Figure 5Aa). DHPG-induced Ca^{2+} transients were abolished by pretreatment with 0 mM Ca^{2+} in the bath solution (2.44 ± 0.74%, n = 10, P < 0.05) (Figure 5Ab) but not by 1 μM thapsigargin (93.17 ± 10.61%, n = 15, P > 0.5) (Figure 5Ac), suggesting that DHPG-induced Ca^{2+} transients are mostly due to an influx of extracellular Ca^{2+} rather than Ca^{2+} release from intracellular Ca^{2+} stores. I next tested whether DHPG-induced Ca^{2+}

transients were associated with TRPV1. DHPG-induced Ca^{2+} transients were completely blocked by the pretreatment with 10 μM capsazepine (2.03 ± 0.18%, n = 14, P < 0.005) (Figure 5Ad), and 100 nM 5'-iodoresiniferatoxin (0.75 ± 0.82%, n = 5, P < 0.005) (Figure 5Ae), which indicated that Ca^{2+} transients can indeed be attributed to Ca^{2+} influx mainly through TRPV1. Further, Ca^{2+} transients were absent in TRPV1$^{-/-}$ mice (Figure 6).

Given that TRPV1 is a non-selective cation channels with high permeability to both Ca^{2+} and Na^+ (Clapham, 2003), I next examined whether DHPG induces TRPV1-mediated inward currents using whole-cell patch clamp recording. When capsaicin-sensitive DRG neurons were exposed to 100 μM DHPG for 10 sec at a holding potential of -60 mV, inward currents were clearly evoked, which was readily reversible and blocked by 10 μM capsazepine (26.47 ± 9.78%, n = 4, P < 0.05) (Figure 5Ba) and 100 nM 5'-iodoresiniferatoxin (12.77 ± 2.21%, n = 5, P < 0.001) (Figure 5Bb). Further, the I-V relationship indicated that DHPG-induced currents have the characteristics of TRPV1-mediated currents with a reversal potential of ~0 mV and a slight outward rectification (Figure 5Bd).

mGluR5 drives DHPG-induced Ca^{2+} entry through TRPV1 channels in sensory neurons

DHPG is a group I mGluRs agonist, and the two subtypes of group I mGluRs, mGluR1 and mGluR5, are both expressed in DRG neurons (Bhave et al., 2001). Thus, I determined the relative contribution of each subtype of mGluRs to DHPG-induced activation of TRPV1. In order to isolate only TRPV1-mediated Ca^{2+} responses produced by the application DHPG, I

eliminated the contribution of intracellular Ca^{2+} stores with 1 μM thapsigargin. Whereas CPCCOEt (50 μM), a mGluR1 specific antagonist, had a slight inhibitory effect (80.52 ± 3.80%, n = 13, $P > 0.002$) (Figure 7Aa), MPEP (50 μM), a mGluR5 specific antagonist, clearly blocked DHPG-induced Ca^{2+} transients (9.15 ± 2.27%, n = 11, $P < 0.001$) (Figure 7Ab). Furthermore, CHPG, a mGluR5 specific agonist, induced Ca^{2+} transients that were similar to DHPG-induced Ca^{2+} transients (74.93 ± 5.85%, n = 10, $P > 0.002$) (Figure 7Ac and 7Ad). Single-cell RT-PCR analysis revealed that all of the DHPG-responsive cells expressed both mGluR5 and TRPV1, whereas mGluR1 expression was homogenous throughout the cells analyzed and was not correlated with the DHPG-induced Ca^{2+} transients in DRG neurons (Figure 7B). These results indicated that DHPG elicits Ca^{2+} influx via TRPV1, primarily through the activation of mGluR5 in capsaicin-sensitive nociceptors.

DHPG-induced Ca^{2+} response results from direct activation of TRPV1 by DAG

Next, I addressed the underlying mechanism for DHPG-induced activation of TRPV1. Since mGluR5 is $G_{q/11}$-coupled receptors linked to phospholipase C (PLC), and the activation of which results in the hydrolysis of $PtdIns(4,5)P_2$ to DAG and inositol-triphosphate (IP_3) (Hermans and Challiss, 2001), I hypothesized that one of the signaling molecules in this pathway was involved in the TRPV1 activation by DHPG. While DHPG-induced Ca^{2+} transients were abolished by 2 μM U73122 (1.74 ± 0.13%, n = 12, $P < 0.001$), a specific PLC inhibitor (the inactive form of 2 μM U73343 had no effect) (Figure 8Aa), DHPG-induced Ca^{2+} transients persisted in the presence of 1 μM staurosporine

30

(89.10 ± 4.20%, n = 9, $P > 0.01$), a non-specific protein kinase inhibitor (Ruegg and Burgess, 1989) or 1 μM bisindolylmaleimide (BIM) (83.50 ± 2.98%, n = 9, $P > 0.001$), a specific PKC inhibitor, and with 1 μM RHC80267, a DAG lipase inhibitor (Figure 8Ab). These results indicated that downstream signaling molecules of PLC mediated DHPG-induced Ca^{2+} transients and that these effects were a result of a protein kinase- and DAG lipase-independent activation of TRPV1, implying that DAG as the most plausible candidate molecule. Indeed, I have recently shown that *1*-oleoyl-2-acetyl-*sn*-glycerol (OAG), a membrane-permeable analogue of DAG, directly activates TRPV1 (Woo et al., 2008). I further found in the present study that bath application of OAG produced a Ca^{2+} transient that was blocked by capsazepine (2.68 ± 0.73%, n = 12, $P < 0.001$), but not by staurosporine and RHC80267 (80.85 ± 3.32%, n = 12, $P > 0.001$) in DRG neurons (Figure 8Ac and 8Ad). I also examined whether OAG could induce inward currents via TRPV1 in DRG neurons. In capsaicin-responsive DRG neurons, 100 μM OAG evoked inward currents (0.20 ± 0.05 nA, n = 6) that were completely blocked by 10 μM capsazepine (Figure 8Ba). Further, the I-V relationship exhibited a typical non-selective cationic current of the TRPV1 response with a reversal potential of ~0 mV and a slight outward rectification (Figure 8Bb). In addition, when I performed cell-attached patch clamp recordings, single channel activities were elicited by 100 μM DHPG, only when applied through the pipette solution, but not when applied through the bath solution. 1 μM capsaicin, applied either through the pipette or the bath solution, elicited higher single channel activities, compared to 100 μM DHPG (Figure 9). These results suggest that the effect of DHPG on TRPV1 is mediated by a membrane-delimited pathway, but not by a diffusible molecule.

31

DAG directly activates the TRPV1 channel in a membrane-delimited manner

I have also demonstrated the mechanisms by which DAG activates TRPV1 using whole-cell patch clamp recording in a heterologous expression system (Woo et al., 2008). To provide further evidences on the membrane-delimited activation of TRPV1, I used Ca^{2+} imaging in the present study. As indicated in the previous study (Woo et al., 2008), one possible mechanism of this pathway would be direct interaction between DAG and TRPV1. To investigate this possibility, I used Y511A mutants of TRPV1 (Jordt and Julius, 2002) transiently expressed in HEK293 cells. This mutant failed to respond to OAG as well as capsaicin (n = 10) (Figure 10A), suggesting that capsaicin and OAG share the Y511 binding site for activation of TRPV1. Alternatively, DAG might produce its effects by replacing $PtdIns(4,5)P_2$ from an inhibitory site on TRPV1 (Prescott and Julius, 2003). Thus, I also examined whether DAG activates TRPV1 in Δ774-838 mutants of TRPV1, which lack a $PtdIns(4,5)P_2$ binding site (786-828) (Ferrer-Montiel et al., 2004). OAG-induced Ca^{2+} transients remained in Δ774-838 mutant, which suggested that this site might not be critical for the activation of TRPV1 by DAG. Normal response to acid stimulus (pH 5.5) of naïve TRPV1, Y551A and Δ774-838 mutants of TRPV1 was used to demonstrate normal functional expression of these constructs in my experimental system (Figure 10B).

I further verified the modulation of TRPV1 by mGluR5 activation in HEK293 cells. To isolate only TRPV1-mediated responses, I examined DHPG-induced Ca^{2+} transients again in the presence of 1 μM thapsigargin. I found that mGluR5 behaved differently depending on the co-expression of TRPV1. DHPG failed to elicit any Ca^{2+} response in either mGluR5-expressing or TRPV1-expressing HEK293 cells. In contrast, DHPG elicited Ca^{2+} response (1.75 ±

32

0.08 ratio, n = 10) that was abolished by capsazepine (0.16 ± 0.01 ratio, n = 10, $P < 0.01$) in HEK293 cells transiently transfected with both mGluR5 and TRPV1 (Figure 11a and 11b). Similar response patterns were observed with 100 µM glutamate as a mGluR5 agonist (Figure 12). These results clearly demonstrated that TRPV1 is trans-activated by mGluR5 to induce Ca^{2+} influx rather than Ca^{2+} mobilization from intracellular Ca^{2+} stores. I also confirmed normal functioning of mGluR5 by evaluating Ca^{2+} mobilization from intracellular stores, observing either Ca^{2+} oscillation or Ca^{2+} transients produced by DHPG without the pretreatment with thapsigargin (Figure 11a inset).

Figure 1. Intrathecal administration of DHPG induces spontaneous pain

A, Spontaneous pain behavior (n = 5) (**a**) and mechanical sensitivity of hindpaws (n = 5) (**b**) were not affected by vehicle injection. Also, there was no discernible difference between in TRPV1 knock-out (open circle) and wild-type (closed circle) mice. **B,** Spontaneous pain behaviors induced by intrathecal administration of DHPG (15 nmol, 5 μl) in TRPV1 knock-out (open circle) and wild type (closed circle) mice. *$P < 0.05$ vs. pre-injection baseline (One-way repeated measure ANOVA followed by Bonferroni *t*-test). n = 6-8; each group.

A

a
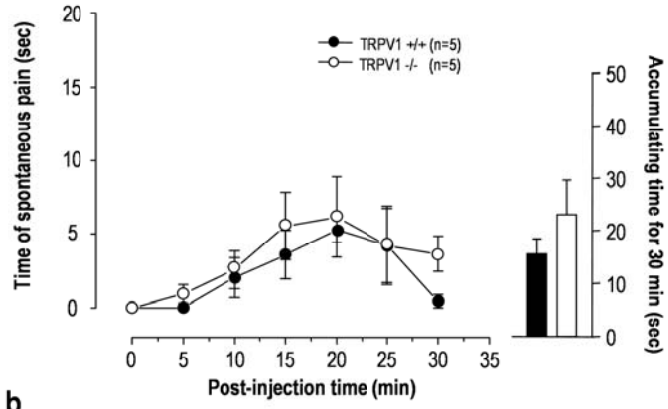
b
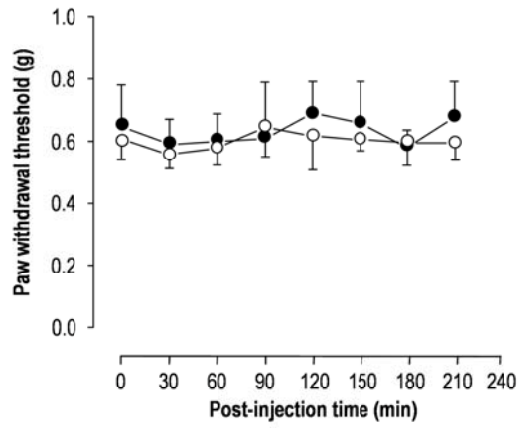
B
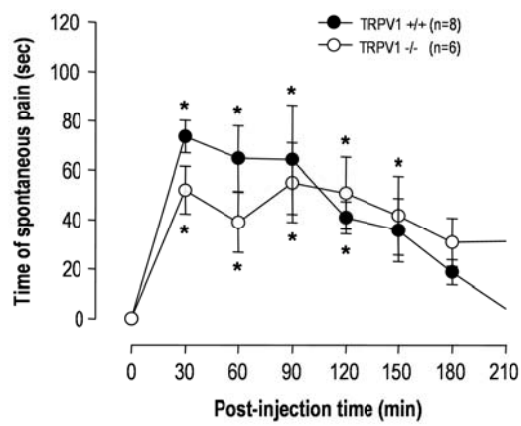
Figure 2. Activation of spinal mGluR5 induces pain behavior

Effects of DHPG (15 nmol, 5 μl, i.t.) on spontaneous pain behavior (n = 5, each group) (**A**) and mechanical sensitivity to von Frey filaments (n = 6-8; each group) (**B**) in both TRPV1 knock-out (open circle) and wild type (closed circle) mice. $**P < 0.001$, $*P < 0.05$ vs. pre-injection baseline (One-way repeated measure ANOVA followed by Bonferroni t-test); $\#\#P < 0.001$, $\#P < 0.05$ vs. wild type mice (Student's t-test).
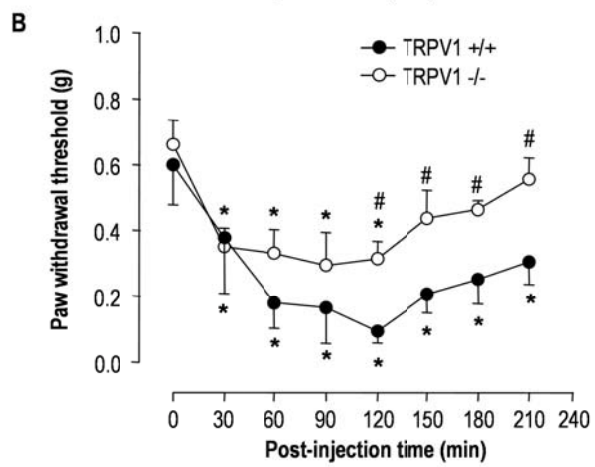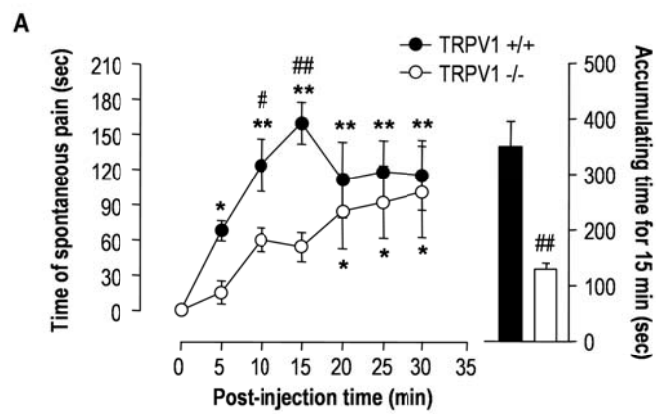
Figure 3. mGluR5 and TRPV1 are coupled on central presynaptic terminals

a, Effects of DHPG on glutamatergic mEPSCs in spinal SG neurons. Traces from a cell before (left) and during 100 μM DHPG (middle, 1 min after the onset of DHPG application), and during 5 μM CZP with 100 μM DHPG (right, 5 min pre-treatment of CZP and 1 min after the onset of DHPG application). CZP indicates capsazepine. **b,** Normalized cumulative probability distributions of the amplitude and the inter-event intervals of mEPSCs. **c and d,** Bar graphs illustrate the percentage change in mean amplitude and frequency of mEPSCs. 6-iodo-CAP: 6-iodonordihydrocapsaicin. (*$P < 0.001$, paired *t*-test versus control, n = 4 and n= 3 respectively). Results are presented as the mean ± SEM.

a Control   DHPG   CZP+DHPG

b

c

d
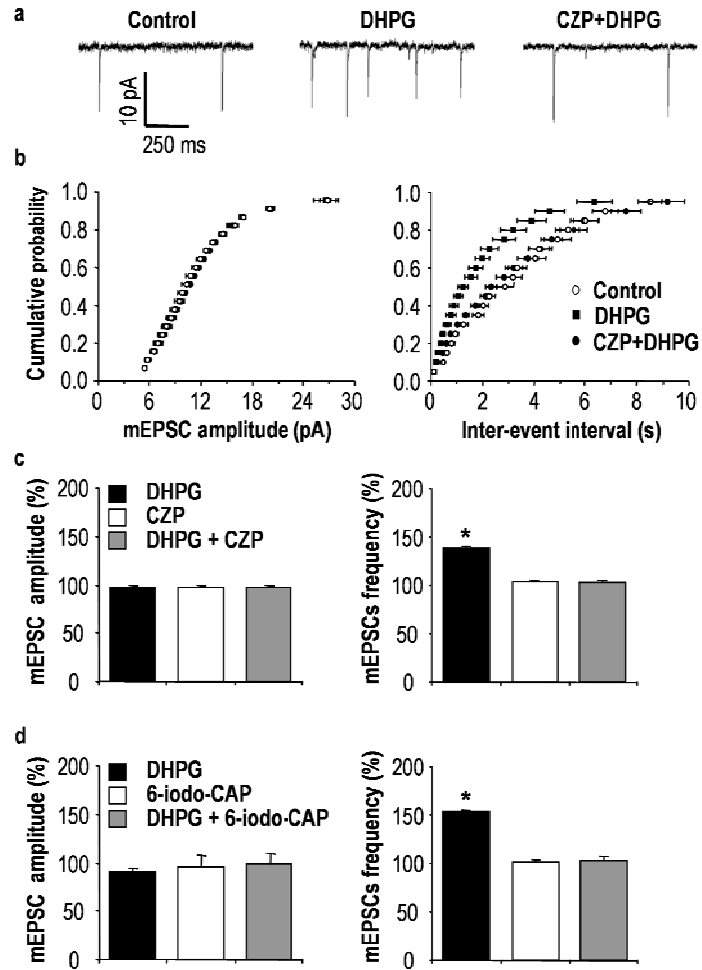
Figure 4. TRPV1 are expressed in axon terminal at the superficial lamina of spinal dorsal horn

An electron micrographic image showing a TRPV1-immunopositive axon terminal in the superficial lamina of spinal dorsal horn at L4 in 10 day old rat. The TRPV1-immunopositive axon terminal contains round vesicles and is apposed to dendrite. The TRPV1-immunoreactivity was usually observed in the axoplasm apart from synaptic site of the axon terminal. The arrow indicates the electron-dense immunoreaction product of TRPV1.
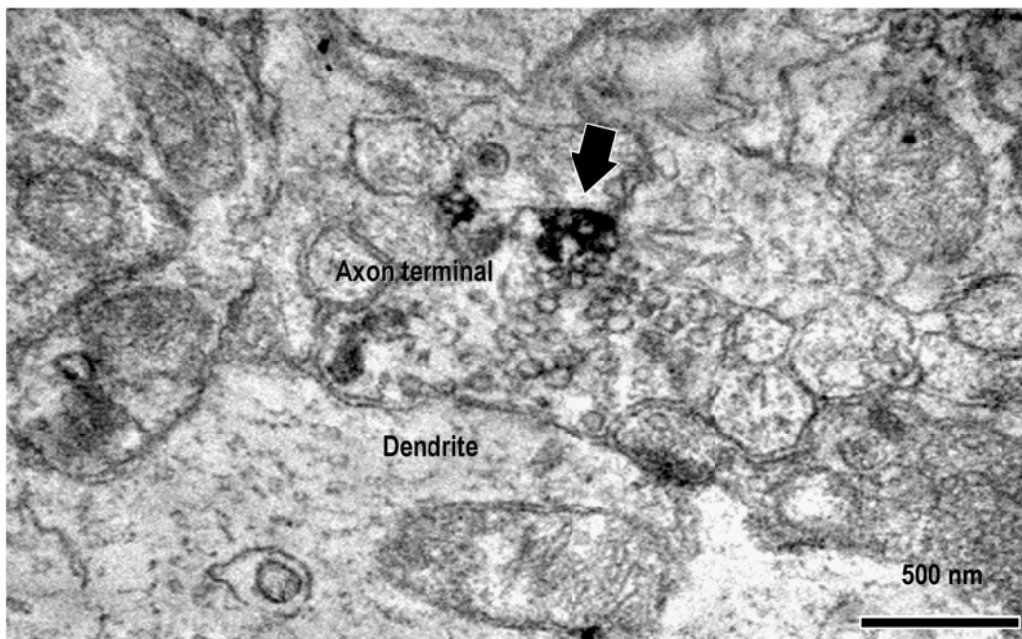
Figure 5. DHPG induces Ca^{2+} transients through TRPV1 in nociceptive sensory neurons

A, Ca^{2+}-transients evoked by sequential application of 100 μM DHPG (n = 12) **(a)** were blocked by extracelluar Ca^{2+}-free condition (n = 10) **(b)** but not by 1 μM thapsigargin (n = 15) **(c)**. DHPG-induced Ca^{2+}-transients were also abolished by 10 μM CZP (n = 14) **(d)** and 100 nM 5'-iodoresiniferatoxin (IRTX, n = 5) **(e)**. CAP indicates capsaicin. Summary of Ca^{2+} response relative to peak amplitude of 1st DHPG response (*$P < 0.05$, paired *t*-test versus 1st DHPG response). Results are presented as the mean ± SEM **(f)**. **B, (a)** Representative DHPG-induced current traces from CAP-sensitive DRG neurons at a holding potential of -60 mV. DRG neurons were repetitively exposed to 100 μM DHPG at 10 min intervals. DHPG-induced currents were abolished by 10 μM CZP (n = 4) **(a)** and 100 nM IRTX (n = 5) **(b)**. **(c)** Summary of the current responses as measured by peak amplitude current, relative to peak amplitude of 1st DHPG response (*$P < 0.05$, paired *t*-test versus 1st DHPG response). Results are presented as the mean ± SEM. **(d)** I-V relationship obtained by a voltage ramp protocol from -100 to +60 mV during DHPG induced current (gray) and before DHPG application (control) exhibited a reversal potential of ~0 mV and a slight outward rectification.

41

A

a

DHPG   CAP

1.0

500 s

b

DHPG

Ca²⁺-free

1.0

400 s

c

DHPG   Thap.

1.0

200 s

d

DHPG   CAP

CZP

0.5

500 s

e

DHPG   KCl

IRTX

0.5

300 s

f

Normalized response
(% of 1st DHPG)

120
100
80
60
40
20
0

*   *   *

☐ 2ⁿᵈ DHPG
■ Ca²⁺-free+DHPG
▨ Thap.+DHPG
▨ CZP+DHPG
▨ IRTX+DHPG

B

a

DHPG   CZP   CAP

100 pA

30 s

1 nA

30 s

b

DHPG   IRTX

50 pA

30 s

c

Normalized response
(% of DHPG)

150

100

50

0

*   *

☐ DHPG
▨ CZP+DHPG
■ Recovery
▨ IRTX+DHPG

d

pA

DHPG
Control
DHPG-Control

500

250

-250

-500

-100   -50   50   100   mV

42
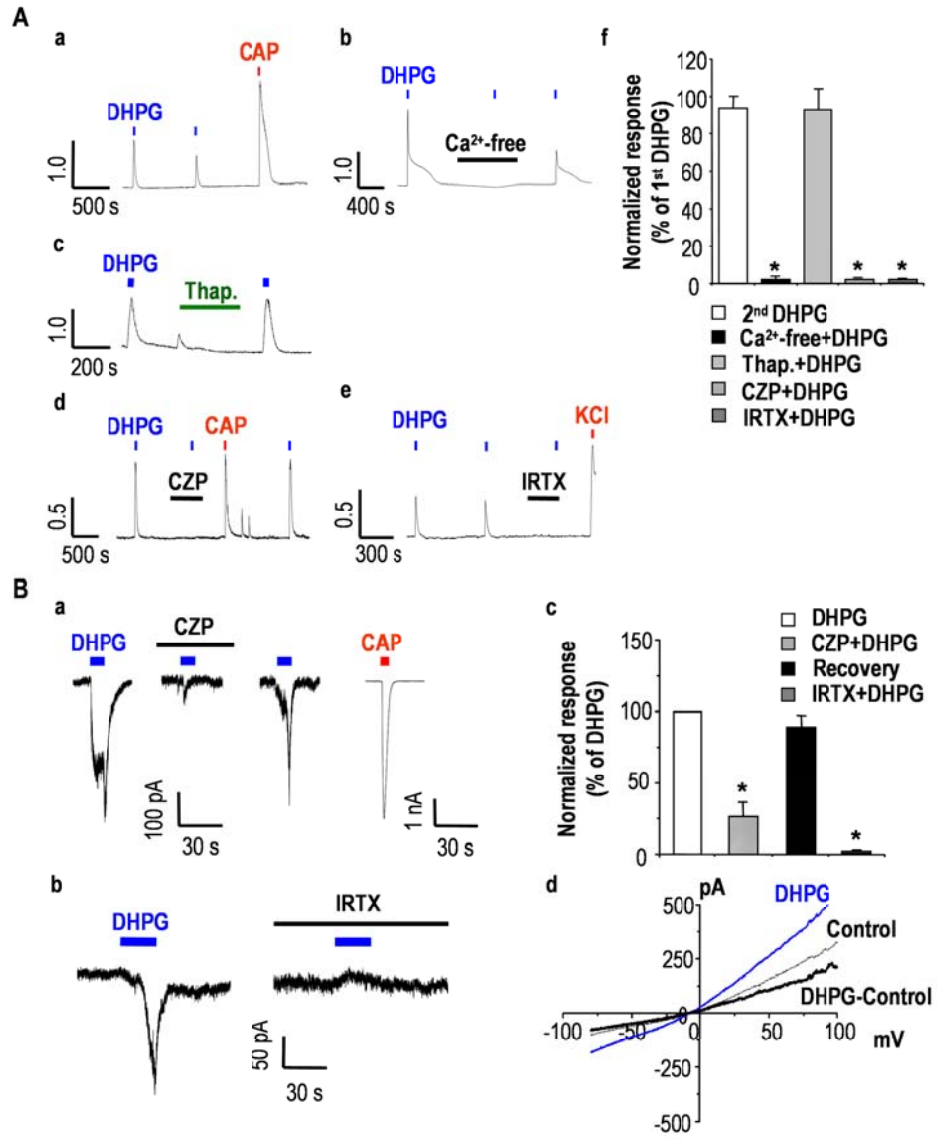
Figure 6. DHPG induced Ca^{2+} transients are absent in $TRPV1^{-/-}$ mice

DHPG-induced Ca^{2+} responses were compared between TRPV1 wild-type and $TRPV1^{-/-}$ mice. Sequential application of 100 μM DHPG elicited Ca^{2+} transients that were abolished by 100 nM IRTX in TRPV1 wild-type mice (2.33 ± 2.25%, n = 15, *P < 0.05). However, 100 μM DHPG either failed to elicit Ca^{2+} transients (n = 15) or just produced Ca^{2+} oscillation in $TRPV1^{-/-}$ mice (n = 3). Cell viability was confirmed by high K^+ (50 mM) at the end of each experiment.

TRPV1 +/+
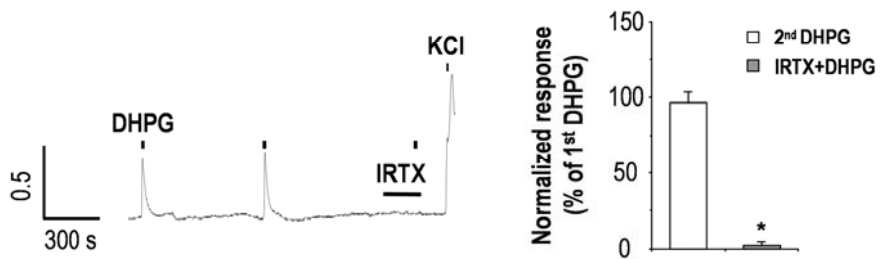
TRPV1 -/-
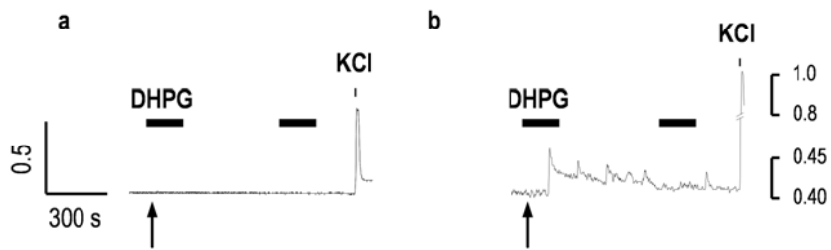
Figure 7. mGluR5 mediates DHPG-induced Ca^{2+} transients in nociceptive sensory neurons

A, DHPG-induced Ca^{2+} transients were not abolished by the mGluR1 specific antagonist, 50 μM CPCCOEt (n = 13) **(a)**, but were abolished by the mGluR5 specific antagonist, 50 μM MPEP (n = 11) **(b)**. $[Ca^{2+}]_i$ transients were also induced by the mGluR5 specific agonist, 300 μM CHPG (n = 10) **(c)**. Summary of Ca^{2+} responses relative to the 1st DHPG response (*$P < 0.001$, paired t-test versus 1st DHPG response). Results are presented as the mean ± SEM **(d)**. **B,** Whole tissue RT-PCR analysis indicated expression of mGluR1 (145 bp), mGluR5 (202 bp) and TRPV1 (330 bp) in DRG neurons. Combination of single-cell RT-PCR following Ca^{2+} imaging (n = 20) revealed an association between coexpression of mGluR5 and TRPV1, and the responsiveness to DHPG and CAP. DRG neurons responsive to both DHPG and capsaicin expressed mGluR1, mGluR5 and TRPV1 (1, n = 8/8), whereas DRG neurons responsive to only capsaicin, but not DHPG, expressed mGluR1 and TRPV1 (2, n = 8/8). DRG neurons unresponsive to DHPG only expressed mGluR1 (3, n = 4/4). The control obtained in bath solution without harvesting cells was negative for all of the tested primers. The three images represent Fura-2 ratio images taken before and during DHPG and CAP applications. Numbers indicate each cell shown in single-cell RT-PCR results. Traces show Ca^{2+} transients in response to DHPG or CAP application.

A

a

Thap.+CPCCOEt

DHPG   CAP

1.0
500 s

b

Thap.+MPEP

DHPG   CAP

1.0
500 s

c

Thap.

DHPG   CHPG   CAP

0.5
200 s

d

Normalized response
(% of 1st DHPG)

□ CPCCOEt+DHPG
▨ MPEP+DHPG
■ CHPG

B

Control   DHPG   CAP

20 μm   1

2

3

1.0
200 s

Ratio (340/380)

2.5

0

DRG tissue   Single cell

1
2
3

β-actin mGluR1 mGluR5 TRPV1   β-actin mGluR1 mGluR5 TRPV1

46
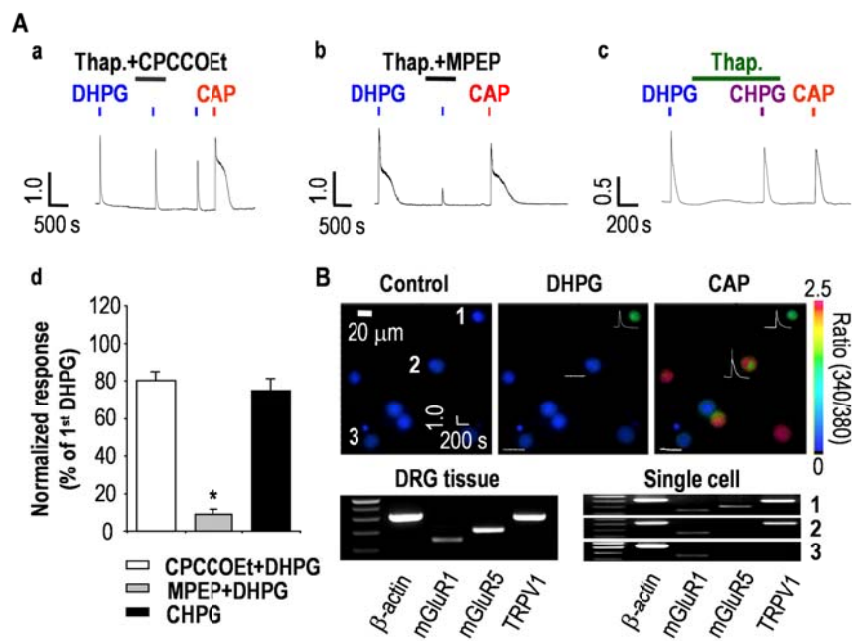
Figure 8. DHPG-induced Ca^{2+} response results from direct activation of TRPV1 produced by DAG

A, DHPG induced Ca^{2+}-responses were abolished by 2 μM U73122 (n = 12), but not by 2 μM U73343 (n = 12) **(a)**. Treatment with either 1 μM staurosporine (SP) or 1 μM bisindolylmaleimide (BIM) with 1 μM RHC80267 (n = 9 each) had no effect on [Ca^{2+}]$_i$ transients by DHPG **(b)**. [Ca^{2+}]$_i$ transients evoked by 100 μM OAG were not affected by 1 μM SP and 1 μM RHC80267 (n = 12), but were abolished by pre-treatment with 10 μM CZP (n = 12) **(c)**. Summary of Ca^{2+} responses relative to the 1st DHPG or OAG response (*$P < 0.001$, paired t-test versus 1st DHPG or OAG response). Results are mean ± SEM **(d)**. **B, (a)** Representative current traces from CAP-sensitive DRG neurons at a holding potential of -60 mV. DRG neurons were exposed to 100 μM OAG twice at 10 min interval (n = 6). OAG-induced currents were abolished by CZP (n = 6). **(b)** I-V relationship obtained by a voltage ramp protocol from -100 to +60 mV during OAG induced current (2) and before OAG application (1) exhibited a reversal potential of ~0 mV and a slight outward rectification.
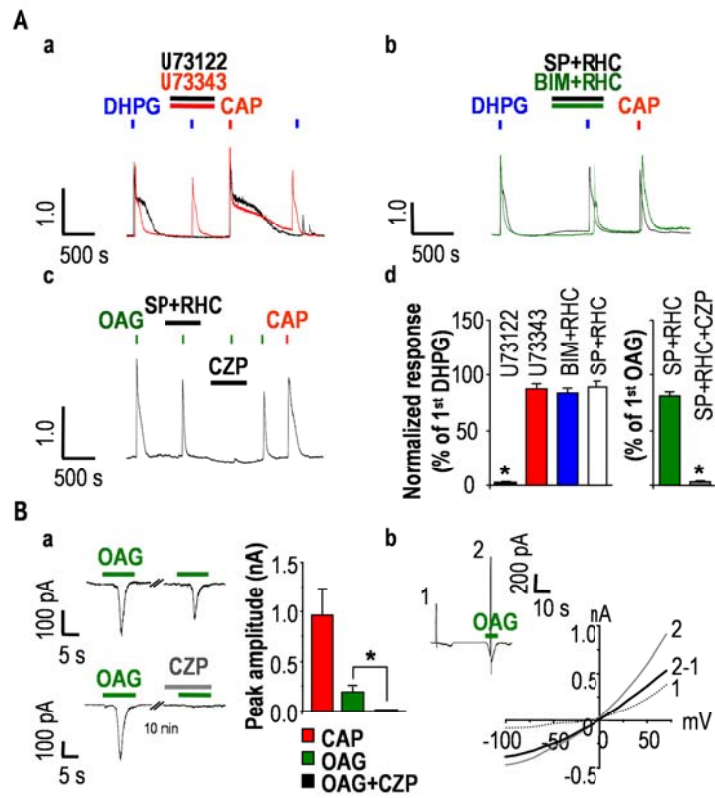
Figure 9. DHPG induced single channel conductance of TRPV1 is mediated by a membrane-delimited pathway

Cell-attached patch clamp recordings at a command potential of +40 mV in DRG neurons. **A**, In the absence of DHPG and capsaicin (CAP), no single channel activities were observed in the experimental condition (**a**) (n = 12 / 12). Single channel activities were not recorded by bath application of 100 μM DHPG (**b**) (n = 5 / 5), but by bath application of 1 μM CAP (**c**) (n = 5 / 7). **B**, Single channel activities were elicited by 100 μM DHPG when applied through the pipette solution (**a**) (n = 6 / 16), and higher single channel activities were observed with sequential bath application of 1 μM CAP in the same DRG neurons (**b**) (n = 6 / 6). **C**, 1 μM CAP included in the pipette solution highly activated single channel currents in DRG neurons (n = 4 / 6). **D**, All-points histogram for channel activities by intra-pipette application of 100 μM DHPG (1.44 $\pm$ 0.01 pA, Po = 0.23) (**a**) and by extracellular application of 1 μM CAP in the same cell (1.40 $\pm$ 0.01 pA, Po = 0.59) (**b**).

A

Control   DHPG   CAP

a   b   c

B

Control   CAP   C

a   b

DHPG   CAP

D

a   b

Intra-pipette DHPG   Intra-pipette DHPG
                            + bath CAP
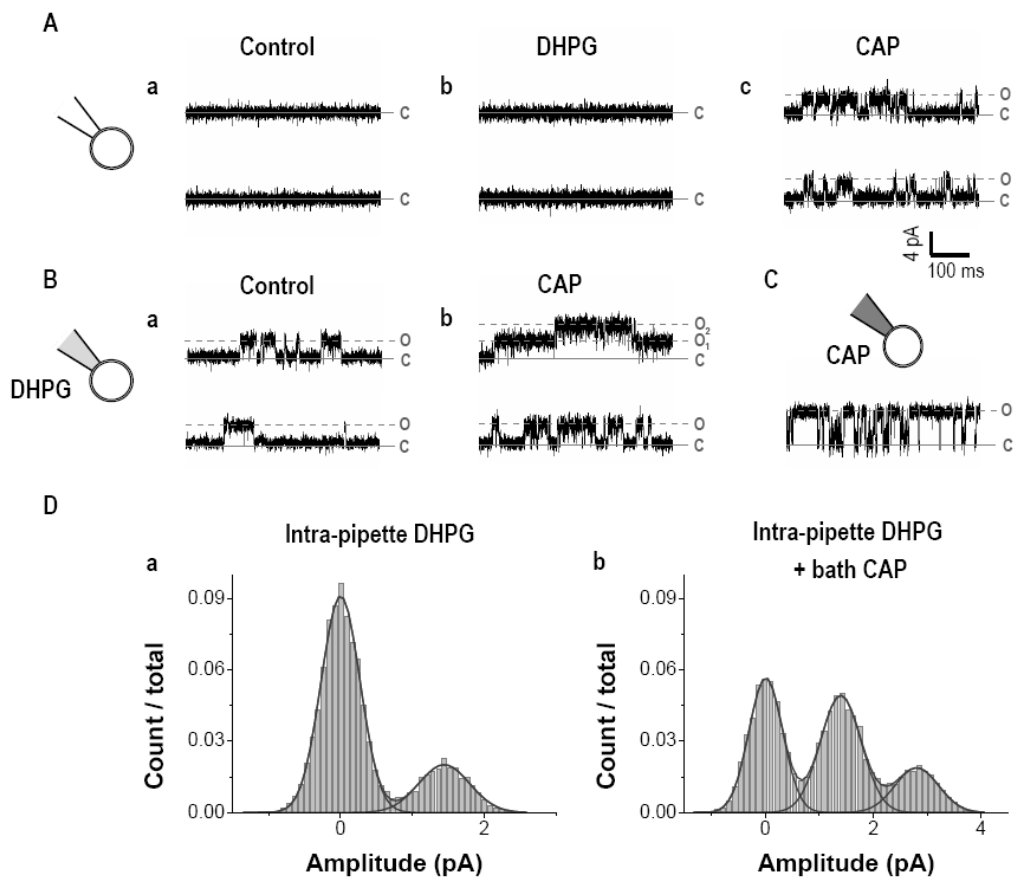
Figure 10. DAG and CAP share their binding site at TRPV1

A, Both OAG and CAP transiently increased $[Ca^{2+}]_i$ in both WT TRPV1- (n = 10) and $\triangle$774-838 mutant-expressing HEK293 cells (n = 10), but not in Y511A mutant-expressing HEK293 cells (n = 10). Results are presented as the mean $\pm$ SEM. **B,** Representative images obtained from Fura-2 based Ca^{2+} imaging experiments in response to CAP, OAG and pH 5.5 from HEK 293 cells transiently transfected with the WT TRPV1, the $\triangle$774-838 mutant and the Y511A mutant.
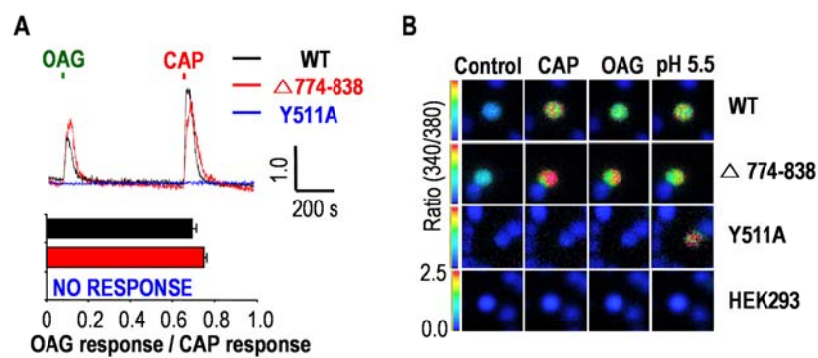
Figure 11. TRPV1 is trans-activated by mGluR5 in HEK 293 cells

a, In the presence of 1 μM thapsigargin, mGluR5-expressing HEK 293 cells had no response to either 100 μM DHPG or 200 nM CAP while TRPV1-expressing HEK 293 cells responded only to 200 nM CAP. In contrast, mGluR5/TRPV1-coexpressing HEK 293 cells were responsive to both 100 μM DHPG and 200 nM CAP which was abolished by 10 μM CZP. DHPG induced typical Ca^{2+}-responses when the cells were not pretreated with thapsigargin (inset). n = 10; each data set. **b**, Summary of DHPG induced-Ca^{2+}-responses in HEK 293 cells as measured by peak amplitude of ratio for each transient (*$P < 0.01$, paired *t*-test versus 1st DHPG response). Results are presented as the mean ± SEM.
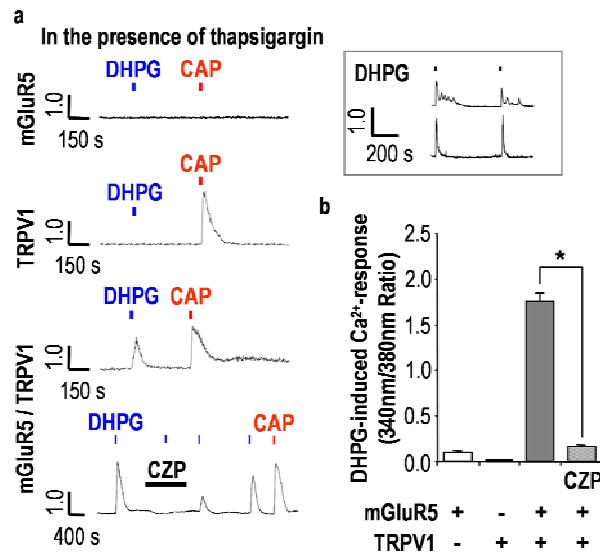
Figure 12. Glutamate induces trans-activation of TRPV1 in mGluR5 / TRPV1-expressing HEK 293 cells

Application of 100 μM glutamate (20 s) induced increments of $[Ca^{2+}]_i$ in mGluR5-expressing HEK 293 cells. These responses were abolished by pretreatment of thapsigargin (5 min), indicating that glutamate-induced Ca^{2+} response in mGuR5-expressing HEK 293 cells was due to a release from intracellular Ca^{2+} stores. However, in mGuR5 and TRPV1-expressing HEK 293 cells, glutamate-induced Ca^{2+} responses were not completely blocked by pretreatment with thapsigargin. The glutamate-induced Ca^{2+} responses in the presence of thapsigargin were blocked by 25 μM 6-iodonordihydrocapsaicin (6-iodo-CAP), a TRPV1 antagonist. Also, TRPV1-expressing HEK 293 cells were sensitive to CAP. Data are presented as the mean ± SEM.

mGluR5

n=65

Glutamate

100 s

Ratio 1

mGluR5

n=10

Glutamate

1 μM Thapsigargin

mGluR5+TRPV1

n=21

Glutamate   1 μM Thapsigargin   1 μM CAP

100 s

Ratio 0.5

mGluR5+TRPV1

n=27

1 μM Thapsigargin pretreatment for 5 min

Glutamate   1 μM CAP

25 μM 6-iodo-CAP

1 μM Thapsigargin

54
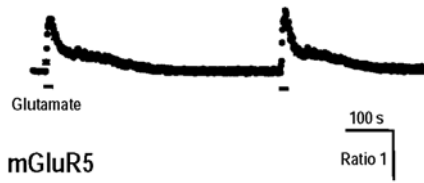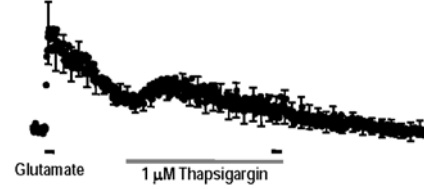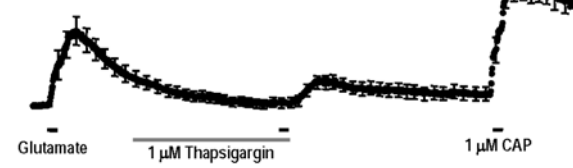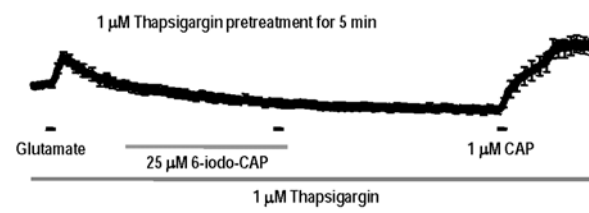
Figure 13. mGluR5 are co-expressed with TRPV1 in DRG neurons

Colocalization of mGluR5 and TRPV1 in cultured DRG neurons. Representative images of mGluR5 (**a**) and TRPV1 (**b**). (**c**) DIC image. (**d**) Merged image shows colocalization of mGluR5 and TRPV1 (thick arrow). Thin arrow indicates mGluR5(+)/TRPV1(-) neurons. Arrow head indicates mGluR5(-)/TRPV1(-) neurons. Scale bar is 30 μm.
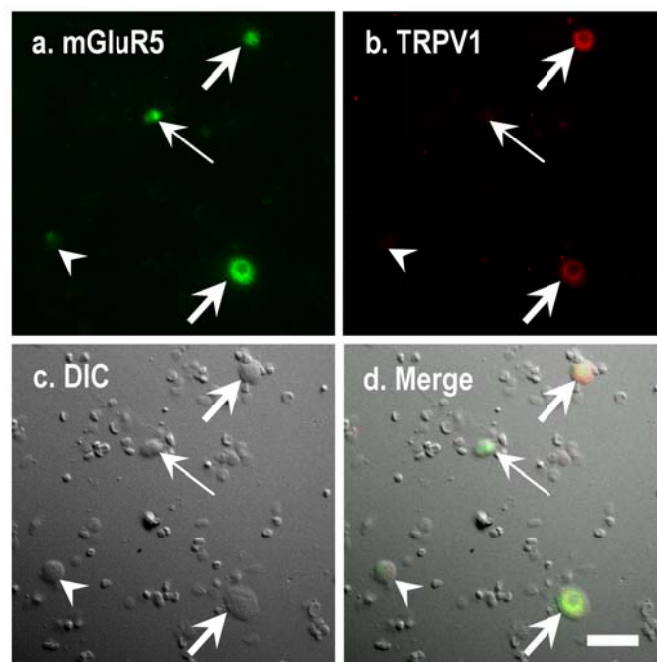
DISCUSSION

I revealed that TRPV1 and mGluR5 are linked in a membrane-delimited manner on the central presynaptic terminals of nociceptive neurons, together serving as presynaptic modulators of nociceptive transmission in the spinal SG area. Spinal TRPV1 is involved in pain behaviors produced by the onset of activation of spinal group I mGluR activation. Given that the enhancement of mEPSC frequency, but not of the amplitude, induced by DHPG was significantly reduced by TRPV1 antagonism, it was believed that coupling of TRPV1 and group I mGluRs on presynaptic terminals could contribute to DHPG-induced pain responses. The *in vitro* results further demonstrated that mGluR5, rather than mGluR1, is coupled to TRPV1, and that DAG produced by the activation of mGluR5 is responsible for mediating the functional coupling of mGluR5 and TRPV1 on presynaptic terminals. Based on my observations, it was thought that cellular mechanisms of spinal presynaptic mGluR5 might be distinct from those of both peripheral mGluR5 and spinal postsynaptic mGluR5. In addition to TRPV1's well-known action as a transducer for pain sensation on the peripheral sensory terminals, it is also highly likely that presynaptic TRPV1, coupled with mGluR5, acts as a Ca^{2+} regulator for synaptic transmission in the SG area.

I found that the effects of mGluR5 activation observed in the calcium imaging and electrophysiology experiments were mediated by TRPV1. Since capsazepine, at micromolar concentrations, is known to produce inhibitory effects on voltage-gated calcium currents (Docherty et al., 1997) in addition to its well-known TRPV1 antagonistic effect, I verified TRPV1-dependent actions

following mGluR5 activation by additionally using structurally different TRPV1 antagonists such as 5'-iodoresiniferatoxin and 6-iodonordihydrocapsaicin. Notably, I also found that the effect of 5-10 μM capsazepine *per se* on mEPSCs was negligible, suggesting the limited effects of capsazepine on voltage-gated calcium currents under my experimental conditions. Absence of Ca^{2+} transients in response to mGluR5 activation in TRPV1$^{-/-}$ mice further revealed TRPV1-specific effects of mGluR5 activation.

Given that the DHPG response was not blocked by the combination of a non-specific protein kinase inhibitor/or PKC inhibitor and DAG lipase inhibitor, DAG produced a response comparable to DHPG, DHPG, only applied into the pipette but not to the bath solution, generated single channel activity, and DAG-induced Ca^{2+} transients were not observed in the capsaicin-binding site TRPV1 mutant, it seems clear that TRPV1 activation by mGluR5 activation occurs via a membrane-delimited generation of DAG. The generation of DAG may be associated with the cellular mechanism for synaptic transmission of nociceptive information in the SG area in the spinal dorsal horn. Although lipid metabolite products such as HPETE and anandamide have been suggested as candidate molecules for mediating GPCR-activation of TRPV1 (Hwang et al., 2000; van der Stelt et al., 2005), the identity of endogenous ligands for TRPV1 at the pathophysiological conditions, especially in the central neurons, are still debated. Recent study demonstrated that DAG is a novel endogenous ligand of TRPV1 (Woo et al., 2008). In the present study, I provide further strong evidence that group l mGluR5 activates the TRPV1 channel in a membrane-delimited manner and DAG mediates functional coupling of group l mGluR5 and TRPV1 on central presynaptic terminals of sensory neurons.

Mechanisms for direct induction of TRPV1 activity by mGluR5 activation in the central presynaptic terminals, which are investigated in this study, seem to be different from those of the enhancement of peripheral TRPV1 function by mGluR5 activation. A previous study demonstrated that activation of mGluR5 on peripheral sensory terminals sensitizes and enhances TRPV1 via PKA and cyclooxygenase pathways (Huang et al., 2002). It is difficult at this point to link these two distinctive *in vitro* results with the appropriate behavioral experiments. However, my experimental finding may reflect differential functional roles of peripheral mGluR5 and central presynaptic mGluR5 in nociceptive signaling. While glutamate, as a key inflammatory mediator released in the periphery after inflammation, acts on mGluR5 for a relatively long period (deGroot et al., 2000), glutamate released from presynaptic terminals may act rapidly on mGluR5 due to the recycling of glutamate to astrocytes via glutamate transporters (Oliet et al., 2001). Therefore, I thought that application of DHPG for short periods of time (20 sec for Ca^{2+} imaging, 10 sec for electrophysiology) rather than 3 min as in a previous study (Huang et al., 2002) would be more appropriate for elucidating the mechanisms of spinal presynaptic mGluR5. Application of DHPG for long periods could mask the effects of membrane-delimited activation of TRPV1 by mGluR5 activation.

Additionally, as previously suggested (Delmas et al., 2002), it is possible that the spatial proximity of receptors (i.e. mGluR5) and target channels (i.e. TRPV1) may determine the specificity of Ca^{2+} responses produced by $G_{q/11}$-coupled receptors which could recruit then either membrane-delimited pathways or downstream pathways inside the cytosol. It remains to be elucidated whether geometrical distances between mGluR5 and TRPV1 are different on peripheral and central nociceptive terminals, and how preferential

functional couplings between different GPCRs and TRP channels are determined at the molecular level.

Group I mGluRs, namely mGluR1 and mGluR5, are distributed on peripheral unmyelinated sensory afferents, in both DRG neurons (Bhave et al., 2001) and spinal dorsal horn (Alvarez et al., 2000). These receptors function such that the activation of peripheral and spinal mGluR1/mGluR5 is sufficient to evoke pain hypersensitivity (Lesage, 2004). However, mGluR1 and mGluR5 may have different cellular mechanisms for their nociceptive signaling. Recent reports demonstrate that mGluR5 is the predominant group I mGluR mediating DHPG-induced responses both in cultured mouse DRG neurons (Huang et al., 2002) and in spinal dorsal horn neurons (Hu et al., 2007). The results also demonstrate that mGluR5 is highly likely to be the predominant group I mGluR on the central presynaptic terminals. Immunohistochemical analysis also revealed double-labeling of DRG neurons with mGluR5 and TRPV1 (Figure 13), which is consistent with the results of a previous report (Walker et al., 2001a).

SG neurons are the first central neurons to relay input from primary afferent neurons (Sugiura et al., 1986). Thus, synaptic modulation of primary afferent neurons in the SG is believed to play an important role not only in acute nociceptive transmission, but also in central sensitization associated with chronic pain (Lu and Perl, 2005). Recently, it has been demonstrated that mGluR5 modulates nociceptive plasticity via Kv4.2 signaling in postsynaptic spinal dorsal horn neurons (Hu et al., 2007). My results suggest that mGluR5 on the central presynaptic terminals of nociceptive neurons may also play an important role for the central sensitization under pathological pain conditions

by membrane-delimited coupling with TRPV1. While presynaptic mGluR5 might be silent in normal physiological pain transmission, mGluR5 present in the perisynaptic area (Jia et al., 1999; Pitcher et al., 2007) could be activated by glutamate spilled over the synaptic cleft following excessive release from central terminals of nociceptive neurons under pathological conditions such as peripheral inflammation and nerve injury. The subsequent Ca^{2+} influx via TRPV1 induced by mGluR5 activation may lead to further glutamate release from central terminals, thereby providing a positive feedback cycle via autocrine function. It has been reported that activation of spinal TRPV1 induced release of substance P (Marvizon et al., 2003) which is necessary for central sensitization of dorsal horn neurons (Ikeda et al., 2003). This observation may be associated with the induction of DHPG-induced pain hypersensitivity documented in the behavioral study.

The present results suggest a plausible cellular mechanism for the contribution of central presynaptic mGluR5 and TRPV1 to nociceptive transmission in the spinal cord. The direct activation of TRPV1 and strong Ca^{2+} signaling induced by DAG following mGluR5 activation implies a previously unknown significant role for TRPV1 as an integrator of multiple $G_{q/11}$-coupled receptors in other areas of the CNS as well as on the central terminals of nociceptive neurons.

CHAPTER 2:

TRPV1 in GABAergic Interneurons Mediates Neuropathic Mechanical Allodynia and Disinhibition of the Nociceptive Circuitry in the Spinal Cord

ABSTRACT

Neuropathic pain and allodynia may arise from sensitization of central circuits. I report a novel mechanism of disinhibition-based central sensitization resulting from long-term depression (LTD) of GABAergic interneurons as a consequence of TRPV1 activation in the spinal cord. Intrathecal administration of TRPV1 agonists led to mechanical allodynia that was not dependent on peripheral TRPV1 neurons. TRPV1 was functionally expressed in GABAergic spinal interneurons and activation of spinal TRPV1 resulted in LTD of excitatory inputs and a reduction of inhibitory signaling to spinothalamic tract (STT) projection neurons. Mechanical hypersensitivity after peripheral nerve injury was attenuated in TRPV1$^{-/-}$ mice but not in mice lacking TRPV1-expressing peripheral neurons. Mechanical pain was reversed by a spinally applied TRPV1 antagonist while avoiding the hyperthermic side effect of systemic treatment.These results demonstrate that spinal TRPV1 plays a critical role as a synaptic regulator and suggest the utility of CNS-specific TRPV1 antagonists for treating neuropathic pain.

INTRODUCTION

Pain hypersensitivity generated by peripheral injury can result from plastic changes in both the peripheral (Campbell and Meyer, 2006; Finnerup et al., 2007) and central nervous systems (Coull et al., 2003; Ikeda et al., 2003; Costigan et al., 2009). Mechanical allodynia, pain response to light touch, is the most common and challenging symptom found in pathological pain (Campbell and Meyer, 2006). The mechanisms underlying induction and maintenance of mechanical hypersensitivity are still uncertain (Costigan et al., 2009) but the dominant population of Nav1.8-expressing peripheral neurons that mediate acute mechanical and thermal pain are not required (Abrahamsen et al., 2008). The transmission of pain signals from primary afferent neurons to higher brain centers is controlled by a balance between excitatory and inhibitory signaling in the spinal cord dorsal horn (Kuner, 2010). A key area for pain processing is the substantia gelatinosa (SG) of the spinal dorsal horn and inhibitory SG interneurons have been proposed as a gate of pain transmission and other sensory modalities to higher brain centers (Melzack and Wall, 1965). It has been suggested that a reduction in tonic and phasic inhibitory control or 'disinhibition' in the spinal dorsal horn is responsible for the amplification of pain messages that produces hyperalgesia and allodynia (Yaksh, 1989; Sivilotti and Woolf, 1994) following peripheral nerve injury (Moore et al., 2002; Basbaum et al., 2009). Thus, central rather than peripheral mechanisms appear to be responsible for the hyperexcitability of nociceptive signaling leading to neuropathic mechanical allodynia (Woolf et al., 1992; Coull et al., 2003; Torsney and MacDermott, 2006; Costigan et al., 2009).

63

TRPV1 antagonists have shown efficacy in animal models of both inflammatory and neuropathic pain (Patapoutian et al., 2009) but systemic administration of TRPV1 antagonists commonly results in hyperthermia caused by peripheral TRPV1 blockade (Steiner et al., 2007). Activation of spinal TRPV1 can generate central sensitization and mechanical allodynia (Patwardhan et al., 2009) and spinal administration of TRPV1 antagonists can attenuate mechanical allodynia induced by nerve injury (Patapoutian et al., 2009) but the cell types or circuits underlying these effects are unknown. Mechanical allodynia associated with TRPV1 activation is unlikely to depend on TRPV1-expressing primary sensory neurons as these are not necessary for the transduction of painful mechanical stimuli (Cavanaugh et al., 2009) and a mechanical pain phenotype is not observed in TRPV1$^{-/-}$ mice (Caterina et al., 2000). Thus the mechanism of action for TRPV1 antagonism in neuropathic mechanical pain relief remains unknown. The expression of TRPV1 in spinal cord SG neurons has recently been suggested (Ferrini et al., 2010). Therefore, I speculated that central TRPV1 may be involved in neuropathic mechanical pain. Here I explored the role of spinal TRPV1 in the spinal cord nociceptive circuitry and further investigated its contribution to the enhancement of mechanical pain sensitivity after peripheral nerve injury.

MATERIALS AND METHODS

All surgical and experimental procedures were reviewed and approved by the Institutional Animal Care and Use Committee (IACUC) at the School of Dentistry, Seoul National University. Animal treatments were performed according to the guidelines of the International Association for the Study of Pain (Zimmermann, 1983). Adult C57BL/6J (wild type) male mice were purchased from Orientbio (Korea) and heterozygous C57BL/6J BAC transgenic male mice expressing EGFP under the control of the GAD65 promoter (GAD65-EGFP mice) (Lopez-Bendito et al., 2004), provided by the Korea Institute of Science and Technology. Animals were housed in a conventional facility with a 12:12 hr light cycle (lights on 8.00am) and ad libitum access to water and chow. Mice were acclimatized for at least one week prior to experiments.

Behavioral studies

For mechanical threshold (von Frey filament) testing, mice were brought from the animal colony and placed in transparent plastic boxes (60 × 100 × 60 mm) on a metal mesh floor (3 × 3 mm mesh). The mice were then left alone for at least 20 min to allow them to acclimate prior to testing. To assess mechanical sensitivities, the withdrawal threshold of the hindpaw was measured using a series of von Frey filaments (0.20, 0.69, 1.57, 3.92, 5.88, 9.80, 19.60 and 39.20 mN, Stoelting, Wood Dale, IL, USA; equivalent in grams to 0.02, 0.07, 0.16, 0.40, 0.60, 1.0, 2.0 and 4.0). The 50% withdrawal threshold was determined

using the up-down method as previously described (Chaplan et al., 1994). A brisk hindpaw lift in response to von Frey filament stimulation was regarded as a withdrawal response. The 0.4 g filament was the first stimulus to be used, and, when a withdrawal response was obtained, the next weaker filament was used. This process was repeated until no response was obtained, at which time the next stronger filament was administered. Interpolation of the 50% threshold was then carried out using the method of Dixon (Dixon, 1980). All behavioral testing was performed by an investigator who was blind to the genetic background of the mice.

Intrathecal injection

Capsaicin (1 μg) and BCTC (10 μg) were dissolved in 0.9% saline using an ultrasonic washer and applied intrathecally. Intrathecal administration was performed as described previously (Hylden and Wilcox, 1980). Briefly, under light enflurane anesthesia (2% in 100% O_2), the vertebral column of mouse was held using the thumb and middle finger of the left hand and the drug was injected intrathecally into each mouse using a 25 μl Hamilton syringe fitted with 31 gauge needle at approximately the lumbar enlargement level of the spinal cord. The injection volume was 5 μl and the injection sites were verified by injecting a similar volume of 1% methylene blue solution and determining the distribution of the injected dye in the spinal cord. Before conducting experiments, the injection method was practiced until the success rate was consistently over 95%.

RTX ablation of peripheral TRPV1-expressing neurons

3 – 4 week old mice were intraperitoneally injected with RTX or vehicle (dissolved in a mixture of 10% Tween 80 and 10% ethanol in normal saline) under isoflurane anesthesia (2% in oxygen) as a single bolus in two injections of 50 μg/kg and 150 μg/kg on days 1 and 2, consecutively. The mice were maintained under isoflurane anesthesia (0.5% in oxygen) for 2 – 3 hour following RTX or vehicle injection. The RTX-treated mice were used in experiments at least 7 days after final RTX injection. Successful depletion of TRPV1-afferent nerves was confirmed by application of a 0.01 mM capsaicin solution to the eye; vehicle-injected mice responded to capsaicin application with 1-2 min vigorous eye wiping, but RTX-injected mice did not. TRPV1 immunoreactivity was reduced in the DRG (Figure 2B) and spinal dorsal horn of RTX-treated mice to levels comparable to TRPV1$^{-/-}$ mice (Figure 2A), reflecting a loss of peripheral and presynaptic receptors, respectively. RTX-treatment also led to a loss of capsaicin-induced sEPSCs in SG neurons (Figure 2C). I further confirmed the efficacy of RTX to functionally eliminate TRPV1 receptors by calcium imaging of isolated DRG neurons. Approximately 63% of DRG neurons from Wt mice but less than 2% of DRG neurons from RTX-treated mice showed a response to capsaicin (Figure 2D).

Real-time RT-PCR

Real-time PCR was performed using a 7500 Real-Time PCR system (Applied Biosystems). Relative mRNA levels were calculated according to the 2-ΔΔCt method (Livak and Schmittgen, 2001). All ΔCt values were normalized

to GAPDH. Real-time RT-PCR experiments were performed at least three times, and the mean ± SEM values are presented unless otherwise noted. The PCR primer sequences used in this study are listed in **Table A**.

Table A. List of DNA primer sequences designed for real-time RT-PCR.

Target gene	Forward primer	Reverse primers	Genbank No.
Mouse GAPDH	5'-ACCTGCCAAGTATGATGACATCA-3'	5'-TGCTGTTGAAGTCGCAGGAGACAA-3'	NM_008084
Mouse TRPV1	5'-GAG GAC CCA GGC AAC TGT GA-3'	5'-TTC CGG CTG GGT GCT ATG-3'	NM_001001445

DRG preparation

DRG neurons obtained from 4 –6-week old mice were prepared. Animals were anesthetized with overdose of isoflurane, decapitated, and DRGs were rapidly removed under aseptic conditions and placed in HBSS (Gibco). DRGs were digested in 1 mg/ml collagenase A (Roche) and 2.4 U/ml dispase II (Roche) in HBSS for 60 min, respectively, followed by 8 min in 0.25% trypsin (Sigma), all at 37°C. The DRGs were then washed in DMEM (Gibco) three times and resuspended in DMEM medium supplemented with 10% FBS (Invitrogen) and 1% penicillin/streptomycin (Sigma). DRGs were then mechanically dissociated using fire-polished glass pipettes, centrifuged (800 rpm, 5 min), resuspended in DMEM medium supplemented with 5% FBS (Invitrogen), 20 ng/ml NGF (Invitrogen), 1× N-2 supplement (Invitrogen), and 1% penicillin/streptomycin (Invitrogen), and plated on 0.5 mg/ml poly-l-ornithine (Sigma)-coated glass coverslips. Cells were maintained at 37°C in a 5% CO_2 incubator.

Ca²⁺ imaging

I performed fura-2 AM-based (Molecular Probes) Ca^{2+} imaging experiments as previously described (Kim et al., 2009a). Briefly, DRG neurons prepared were loaded with fura-2 AM (2 μM) for 40 min at 37°C in a balanced salt solution [BSS; containing (in mm) 140 NaCl, 5 KCl, 2 $CaCl_2$, 1 $MgCl_2$, 10 *N*-[2-hydroxyethyl]piperazine-*N'*-[2-ethanesulfonic acid] (HEPES), 10 glucose, adjusted to pH 7.3 with NaOH]. The cells were then rinsed with DMEM and incubated in DMEM for an additional 20 min to de-esterify the dye. Cells on slides were placed onto an inverted microscope and illuminated with a 175 W xenon arc lamp; excitation wavelengths (340/380 nm) were selected by a monochromator wavelength changer. Intracellular calcium concentrations ($[Ca^{2+}]_i$) were measured by digital video microfluorometry with an intensified charge-coupled-device camera (CasCade, Roper Scientific) coupled to the microscope and a computer with Metafluor software (Universal Imaging). All drugs were applied via bath perfusion at a flow rate of 5 ml/min.

Electron microscopy

C57BL6 mice (male, 6 week-old) were deeply anesthetized with sodium pentobarbital (80 mg/kg, i.p.) and perfused transcardially with 4% paraformaldehyde in 0.1 M phosphate buffer, (PB; pH 7.4). The brainstem and L4 DRG were removed and cut transversely on a vibratome at 60 μm. The sections were post-fixed in the mixture of 4% paraformaldehyde and 0.01% glutaraldehyde in 0.1 M PB for 30 min at 4 °C and then cryoprotected in 30 %

sucrose in PB overnight at 4 °C. Sections were frozen on dry ice for 20 min and thawed in phosphate buffered saline (PBS; 0.01M, pH 7.2) to enhance penetration of antibody, blocked with 3% H_2O_2 for 10 min to suppress endogenous peroxidases, and with 10% normal donkey serum (NDS; Jackson Immunoresearch, West Grove, PA, USA) for 30 min to mask secondary antibody binding sites. For double immunostaining for TRPV1 and GAD, sections of L4 DRG pretreated as above were incubated overnight in a mixture of goat anti-TRPV1 (1:500; Santa Cruz Biotechnology, Santa Cruz, CA) and mouse anti-glutamic acid decarboxylase 65/67 (GAD65/67, a marker for GABAergic neurons; dilution 1:1,000; Stressgen Biotechnologies) antibodies. After rinsing in PBS, sections were incubated with a mixture of biotinylated donkey anti-goat (1:200, Jackson Immunoresearch) and gold-conjugated donkey anti-mouse (1:50; EMS, Hatfield, PA, USA) antibodies for 2 hour. The sections were post-fixed with 2% glutaraldehyde in PB for 10 min, rinsed in PBS several times and incubated for 4 min in silver intensification solution (HQ silverTM Enhancement Kit, Nanoprobes, USA) and rinsed in 0.1 M sodium acetate and PB. The sections were then incubated with ExtrAvidin peroxidase (1:5,000; Sigma, St. Louis, MO, USA) for 1 hour, and the immunoperoxidase was visualized by nickel-intensified 3.3'-diaminobenzidine tetrahydrochloride (DAB). Sections were further rinsed in PB, osmicated (0.5% osmium tetroxide in PB) for 1 hour, dehydrated in graded alcohols, flat embedded in Durcupan ACM (Fluka, Buchs, Switzwerland) between strips of Aclar plastic film (EMS), and cured for 48 hour at 60 °C. The sections were cut with diamond knife, collected on formvar coated single slot nickel grids and stained with uranyl acetate and lead citrate. Grids were examined on a Hitachi H-7500 electron microscope (Hitachi, Tokyo, Japan) at 80 kV accelerating voltage. Images were

captured with a DigitalMicrograph software driving a cooled CCD camera (SC1000; Gatan, Pleasanton, CA, USA) attached to the microscope, and saved as TIFF files.

DRG immunohistochemistry

Naïve (n=3) and RTX-treated C57BL/6 mice (n=3) were deeply anaesthetized with sodium pentobarbital (100 mg/kg i.p.) and perfused transcardially with heparinised saline (500 U/l) followed by Zamboni fixative (4% paraformaldehyde, 2% picric acid, pH 7.4). Bilateral L4 and L5 DRG were removed and cryoprotected in a 30% sucrose PBS solution overnight. DRG from mice of both groups were frozen embedded together and cryosections (14 μm) were cut and thaw mounted to Superfrost slides. After blocking for one hour at room temperature (5% normal donkey serum, 0.1% triton-X 100) sections were probed with guinea pig anti-TRPV1 (1:1000) (Chemicon) overnight at 4°C followed by FITC–conjugated donkey anti-guinea pig (1:200) (Jackson) for 1 hour at room temperature in PBS (pH 7.6). Images were captured with a confocal microscope (Olympus FV-300, Japan) with identical acquisition parameters.

Slice preparation of mouse spinal cord

I used adult (4 - 6-week old) C57BL/6J (wild type) male mice and heterozygous C57BL/6J BAC transgenic male mice expressing EGFP under the control of the GAD65 promoter (GAD65-GFP mice) (Lopez-Bendito et al., 2004). Mice were deeply anesthetized with excess isoflurane, and the spinal

cord including lumbosacral enlargement was exposed by a dorsal laminectomy. Dissected tissue blocks were placed into ice-cold cutting solution containing (in mM): 245 sucrose; 3 KCl; 6.0 $MgCl_2$; 0.5 $CaCl_2$; 26 $NaHCO_3$; 1.25 NaH_2PO_4; 11 glucose; 5 HEPES; 1.0 Kynurenic acid (pH 7.4, when bubbled with 95% O2 / 5% CO2). Transverse slices (300 μm) were prepared using vibroslicer (Lieca VT1000 Plus, Leica Microsystems GmbH, Germany). The slices were collected in a slice chamber containing recording artificial cerebrospinal fluid (aCSF) composed of (in mM): 126 NaCl; 3 KCl; 1.3 $MgCl_2$; 2.5 $CaCl_2$; 26 $NaHCO_3$; 1.25 NaH_2PO_4; 11 glucose; 5 HEPES (pH 7.4, when bubbled with 95% O2 and 5% CO2 and had osmolarity of 305 - 310 mOsmol.). The slices were initially maintained at 32 °C for 45 min to recover and transferred to the slice chamber kept at room temperature (25 ± 1 °C) until used.

Single-Cell Reverse Transcription-Polymerase Chain Reaction (single-cell RT-PCR)

Single-cell RT-PCR was performed as previously described (Park et al., 2006). Briefly, under fluorescence microscopy, GAD65-GFP SG neurons and DiI labeled STT neurons were verified from the slice prepared. Identified cells were harvested into a patch pipette with a tip diameter of about 20 μm, gently put into a reaction tube containing reverse transcription reagents, and incubated for 1 hour at 50 °C (superscript III, Invitrogen). All PCR amplifications were performed with nested primers (**Table B**). The first round was performed in 20 μl PCR premix (Bioneer) reaction buffer containing 0.2 μM "outer" primers and 3 μl RT product. The protocol included 5 min of initial denaturation at 95 °C, followed by 35 cycles of 40 s of denaturation at 95 °C, 40 s of annealing at

55 °C, and then 40 s of elongation at 72 °C, and was completed with 7 min of final elongation. The second round reaction protocol was the same as the first round using "inner" primers and 1.5 μl first round products. PCR products were then visualized on ethidium bromide-stained, 1.2% agarose gels.

Table B. List of DNA primer sequences designed for single-cell RT- PCR.

Target gene (Product length)[a]	Outer primers	Inner primers	Genbank No.
β-actin (326 bp, 231 bp)	5'- CATCACTATTGGCAACGAGCG-3' 5'- ACATCTGCTGGAAGGTGGACAG-3'	5'- GGCTCTTTTCCAGCCTTCCTT-3' 5'- CCACCGATCCACACAGAGTACT-3'	NM_007393
TRPV1 (352 bp, 249 bp)	5'- CATGCTCATTGCTCTCATGG-3' 5'- AACCAGGGCAAAGTTCTTCC-3'	5'- CATGGGCGAGACTGTCAAC-3' 5'- CTGGGTCCTCGTTGATGATG-3'	NM_001001445

[a] (n, n) indicates product size obtained from outer and inner primers, respectively.

Visualized whole-cell patch clamp recordings

The slices were transferred to a recording chamber mounted on the stage of a BX50WI microscope (Olympus, Tokyo, Japan) fitted with fluorescence optics and a 40X water immersion objective. Slices were continuously superfused (~5 ml/min) with recording aCSF. Wild-type SG neurons, GAD65-GFP SG neurons and STT neurons were visualized with fluorescence microscope linked to a Luca Andor camera (Andor Technology plc) under control of metaflour processing system (Universal Imaging). The data were recorded and acquired using an EPC-10 amplifier (HEKA, Germany) and Pulse 8.30 software (HEKA, Germany). Identified SG neurons in translucent area of lamina II and visualized STT neurons were recorded using microelectrodes of 5 – 8 MΩ pulled from borosilicate capillaries (World Precision Instruments) on a Narishige puller (PP-830, Narishige, Japan). Whole-cell patch clamp recordings were performed at

room temperature (25 ± 1 °C). Capsaicin-induced currents were recorded using an internal solution containing (mM); 136 K-gluconate; 10 NaCl; 1 $MgCl_2$; 10 EGTA; 10 HEPES; 2 Mg-ATP; 0.1 Na-GTP (pH 7.33 with KOH, 291 mOsmol) and modified aCSF of the following composition (mM): 126 NaCl; 3 KCl; 6 $MgCl_2$; 0.0 $CaCl_2$; 26 $NaHCO_3$; 1.25 NaH_2PO_4; 11 glucose; 2 EGTA (pH 7.4, when bubbled with 95% O2 and 5% CO2 and had osmolarity of 305 - 310 mOsmol). To prevent spontaneous synaptic activity, a cocktail of neurotransmission inhibitors were added (in μM): 10 CNQX; 50 D-APV, 10 picrotoxin, 2 strychnine, 0.5 tetrodotoxin. Firing pattern of action potentials, resting membrane potential and cell capacitances were measured within 1 min after attaining whole-cell configuration. To record evoked excitatory postsynaptic currents (EPSCs), SG neurons were held at -70mV and recording pipettes were filled with an internal solution containing (in mM); 130 K-gluconate; 8 NaCl; 0.5 EGTA; 10 HEPES; 4Mg-ATP ; 0.3 Na-GTP; 5 QX-314 (pH 7.31 with KOH, 270 mOsmol). Electrical stimuli (0.01 ms, 0.066 Hz) were delivered through a bipolar, Teflon-coated tungsten electrode, which was placed in dorsal root entry zone of spinal cord and monosynaptic EPSCs were identified on the basis of the absence of conduction failure of evoked EPSCs. To determine the paired-pulse ratio before and after drug application, two EPSCs were evoked by a pair of stimuli given at 50 ms intervals (Tominaga et al., 1998). The paired-pulse ratio was presented as the ratio of the amplitude of the second synaptic response to the amplitude of the first synaptic response. The amplitude of evoked EPSCs was measured, four consecutive currents were averaged, and these measurements were expressed relative to the normalized baseline. To record evoked inhibitory postsynaptic currents (IPSCs) from STT neurons, the DiI labeled neurons were held at 0 mV and recording micropipettes

74

were filled with an internal solution containing (in mM); 125 K-gluconate; 4 NaCl; 0.5 $CaCl_2$; 2 $MgCl_2$; 5 EGTA; 5 HEPES; 4 Na_2-ATP; 5 QX-314 (pH 7.38 with KOH, 283 mOsmol). Electrical stimuli protocol was the same as evoked EPSCs recordings.

Western blotting analysis of GluA2 receptors (GluR2) in membrane fraction

Spinal cord slices (700 μm) were incubated in 95% O_2/5% CO_2 saturated recording aCSF with 5 μM capsaicin for 10 min at 32 °C. After treatment of capsaicin, the slices were washed out for 30 min. For subcellular fractionation, the spinal cord slices were homogenized in homogenizing buffer containing 10 mM Tris-HCl, 5 mM EDTA, 300mM sucrose, PIC (Sigma-Aldrich), pH 7.5 on ice. The homogenates were centrifuged at 1000 g for 10 min at 4 °C and then 30% of the supernatant was collected for total protein. After centrifugation at 20000 g for 20 min at 4 °C, the supernatant (S2) was collected for cytosolic proteins. The pellet (P2) was resuspended in homogenizing buffer to obtain membrane fraction. Protein concentration was determined with BCA assay kit (Pierce) and quantified with a plate reader. Each samples of 50 μg were mixed with 6x SDS sample loading buffer followed by boiling for 5 min. After measurement of protein concentration using BCA assay, the proteins were separated on 5% stacking/8% resolving gels by SDS-PAGE and then transferred onto PVDF membrane. The membrane was blocked with 5% BSA or 5% non fat skim milk in TBS containing 0.1% Tween20 (TBS-T), pH 7.4 for 1 hour at room temperature and subsequently incubated with rabbit anti-GluR2 (Milipore, 1:1000), rabbit anti-N cadherin (Milipore, 1:10000), mouse anti-β-actin (Sigma, 1:10000) at 4 °C overnight. The membrane was washed with TBS-T and then

incubated with horseradish peroxidase conjugated goat anti-mouse IgG, goat anti-rabbit IgG secondary antibody respectively for 1 hour at room temperature. After incubation, the membrane was washed with TBS-T then exposed to x-ray film by chemiluminescence reagent (West-zol, Intron). For the analysis of the visualized band, each band was quantified with Las-1000 (multi Gauge V3.0). Independent experiments were repeatedly conducted.

Application of retrograde tracer into VPL region of thalamus

Experiments were carried out on C57BL/6J (4-week old) male mice as previously described (Kim et al., 2009a). Mice were anesthetized with pentobarbital sodium (40 mg/kg). After placing a mouse in a stereotaxic apparatus (Narishige, Tokyo, Japan), a small scalp cut was made. A hole was drilled into the skull to allow the insertion of the needle on a 50 μl Hamilton syringe into the target area. Then a red fluorescent dye (1,1′-dioleyl-3,3,3′,3′-tetramethulindocarbocyanine methanesulfonate [Δ9-DiI], Molecular Probes; 1 μl, 25 mg/0.5 ml in ethanol) was injected into the region of VPL of the thalamus (Bregma: -1.2 ± 0.2 mm, midline: 1.9 ± 0.2 mm, depth: 3.2 ± 0.2 mm) using a glass micropipette (20 μm tip diameter). The tracer injection was monitored under a stereomicroscope. The incision was closed after the injection. Animals were returned to their cages for 5 – 8 days, which was sufficient to permit the retrograde tracer to be transported to the soma of the STT neurons. DiI-labeled STT neurons were observed in deep lamina of spinal cord.

Chronic constriction injury (CCI) model

Mice (6 – 8 weeks old) were anaesthetized by enflurane (4% induction; 2-3% maintenance) at 3 L/min in O_2 via a face mask. The right thigh was shaved, iodine treated and an incision made parallel to the femor. The muscle was parted by blunt forcep dissection to expose the sciatic nerve proximal to the trifurcation. Two silk sutures (7-0; Ailee Co. Ltd, Busan, Korea) were tied loosely around the full circumference of the sciatic nerve 2-3 mm apart and secured with a reef knot. Care was taken for the sutures to lie adjacent to but not visibly compressing the nerve; intraneural blood flow was not impeded. The wound was closed in two layers, with silk sutures (for muscle fascia) and an autoclip (for skin). Aseptic conditions were maintained throughout. Surgery was performed blind to the treatment-group and genotype of the mice and alternated between cages. For reversal of chronic mechanical allodynia, BCTC was injected intrathecally 28 days after CCI surgery.

Rectal temperature recording

Rectal temperature was measured by insertion of a flexible bead probe with a digital thermometer (TC-324B, Warner Instrument Corp., Hamden, CT, USA) while mice were briefly restrained by the handler; the meter reading was equilibrated for 10 s. Temperature recordings were carried out between 12 p.m. and 3 p.m. The ambient room temperature was maintained between 22 ~ 24°C. Baseline rectal temperature was measured at least twice before dosing and 0.25, 0.5, 0.75, 1, 1.5, 2 hours after dosing. For intravenous (i.v.) injection mice were placed in standard restraining device, tail was swabbed with alcohol and injected with 0.04 ml of either drug or vehicle (50% DMSO in sterile saline) into the lateral tail vein. The method for intrathecal (i.t.) injection was as for

behavior testing (see above).

Drug application

Capsaicin, AMPA (α-amino-3-hydroxyl-5-methyl-4-isoxazole-propionate); agonist for AMPA receptor, 6-iodonordihydrocapsaicin; TRPV1 antagonist, D-AP5; NMDA receptor antagonist, picrotoxin; $GABA_A$ antagonist, strychnine; glycine receptor antagonist, L-703,606; neurokinin 1 receptor antagonist and QX-314; membrane-impermeable Na_v channels blocker were purchased from Sigma-Aldrich (St. Louis, MO). CNQX; AMPA receptor antagonist; Hexyl-HIBO; Group I mGluR antagonist, LY341495; Group II mGluR antagonist, and TTX; Na_v channels blocker were were purchased from Tocris (Buckhurst Hill, United Kingdom). BCTC; TRPV1 antagonist was from SK biopharmaceuticals (Korea). (RS)-α-methyl-4-carboxyphenylglycine (MCPG); non-selective group I and group II mGluR antagonist was purchased from Ascent Scientific (Bristol, United Kingdom). Capsaicin was prepared from 10 mM stock solution in ethanol and applied using local perfusion system located to 1 - 2 mm from the slice. AMPA was delivered through a glass puffer pipette (1 µm tip diameter, ~10 psi, 69 kPa) using a pneumatic PicoPump (Picospritzer III). The tip of the puffer pipette was positioned to a point about 20 - 30 µm from recorded cell soma. Cocktail of the inhibitors was applied by superfusion with modified aCSF. All drugs exclude above indicated were made as stock solutions and keep at -20 °C and diluted as final concentration (1:1000 - 5000).

Statistical Analyses

78

I expressed data as mean ± standard error (SEM), unless otherwise indicated. Percentages of SG neurons expressing TRPV1 mRNA were compared using a Fisher's exact test. Significances in 50% paw withdrawal thresholds in comparison with pre-injury levels were calculated by one-way repeated measure analysis of variance (ANOVA) followed by Bonferroni's post-test and Student's unpaired t-test. Mechanical hypersensitivity was calculated by the percentage difference in the mechanical thresholds of ipsilateral and contralateral hind paws accumulated from each time point up to 28 days after CCI. The anti-nociceptive effect of BCTC after intrathecal injection was calculated as a percentage of the maximum potential effect (MPE) relative to pre-injury baseline threshold. Whole-cell current amplitudes after drug application were compared to pre-drug baseline by Student's paired t-test. Expression level of TRPV1 mRNA and protein were compared by Student's unpaired t-test. The data were analyzed and plotted using Origin Pro 8 (Microcal Software, Inc) and GraphPad Prism 5 (GraphPad Software, Inc).

RESULTS

Spinal TRPV1 Activation in SG Neurons Produces Mechanical Allodynia

I first examined the relative contribution of peripheral and central TRPV1 to the development of mechanical allodynia induced by the TRPV1 agonist capsaicin. Consistent with a recent report (Patwardhan et al., 2009), intrathecal administration of capsaicin in mice decreased the paw withdrawal mechanical threshold (Figure 14A). This effect was prevented by co-administration of the TRPV1-selective antagonist N-(4-tertiarybutylphenyl)-4-(3-chloropyridin-2-yl) tetrahydropyrazine-1(2H)-carbox-amide (BCTC, Figure 14A). Capsaicin had no effect on mechanical thresholds in TRPV1$^{-/-}$ mice (Figure 14B). Intrathecal capsaicin could act on either postsynaptic TRPV1 expressed in spinal cord neurons or on presynaptic TRPV1 expressed at the primary afferent terminals of sensory neurons. To distinguish between these possibilities I generated mice in which TRPV1-expressing peripheral neurons are ablated by intraperitoneal injection of the ultra-potent TRPV1 agonist resiniferatoxin (RTX). RTX treatment eliminated TRPV1 mRNA in dorsal root ganglia without altering mRNA levels in the spinal cord (Figure 14C). RTX treatment appeared to be effective in completely ablating peripheral neurons expressing TRPV1, including their central terminals, because there was complete loss of TRPV1 immunoreactivity in DRG neurons (Figure 15A and 15B), nearly complete (98%) loss of capsaicin-induced calcium increases in DRG cell bodies (Figure 15D), and complete loss of capsaicin response of presynaptic terminals (Figure 15C). However, in contrast to TRPV1$^{-/-}$ mice, intrathecal capsaicin injection was still able to effectively induce mechanical hypersensitivity in RTX-treated

80

mice (Figure 14B), suggesting a site of action on central neurons. High resolution electron microscopic analysis of the lumbar spinal cord revealed TRPV1 was localized not only to presynaptic terminals, as expected (Figure 14D), but also to postsynaptic dendrites in the dorsal horn (Figure 14E), and postsynaptic cell soma (Figure 14F). No TRPV1 immunoreactivity was observed in the dorsal horn of TRPV1$^{-/-}$ mice (Figure 14G).

TRPV1 Is Functionally Expressed by GABAergic SG Neurons

I next sought to identify the population of postsynaptic spinal cord neurons that functionally express TRPV1. SG neurons of the spinal dorsal horn are a heterogenous population of interneurons (Todd and McKenzie, 1989; Maxwell et al., 2007) that receive direct inputs from primary afferent fibers (Yasaka et al., 2007). TRPV1 immunoreactivity was co-localized in postsynaptic dendrites with the GABA synthesizing enzyme glutamic acid decarboxylase 65 (GAD65) (Figure 16A). TRPV1 mRNA was detected in 76.7% of GAD65-enhanced green fluorescent protein (EGFP) positive SG neurons by single-cell RT-PCR (Figure 16B, *upper*). In contrast, the occurrence of TRPV1 mRNA in GAD65-EGFP negative SG neurons was lower (25%, Figure 16B, *lower*). To test for functional expression of TRPV1, I applied capsaicin (CAP) to spinal cord slices while recording from SG neurons. In addition to eliciting spontaneous excitatory postsynaptic currents (EPSCs), as expected from activation of presynaptic TRPV1 (Figure 17A), capsaicin also elicited clear whole-cell currents in SG neurons (Figure 17B) that persisted in the presence of a cocktail of neurotransmission blockers including 6-cyano-7-nitroquinoxaline-2,3-dione (CNQX), amino-5-phosphonovaleric acid (AP5), picrotoxin, strychnine and

81

tetrodotoxin with high MgCl$_2$ and a calcium chelator (see Materials and Methods). Whole-cell capsaicin-induced currents (16.5 ± 2.5 pA) were recorded in identified GAD65-positive SG neurons; these currents were blocked by the TRPV1 antagonist 6-iodo-nordihydrocapsaicin (6-iodo-capsaicin, 18.70 ± 1.47%, Figure 16C) and showed outward rectification with a reversal potential of ~0 mV characteristic of TRPV1-mediated currents (Caterina et al., 1997) (Figure 16D and Figure 17C). A high proportion of these functionally TRPV1-positive, GAD65-positive SG neurons displayed a long-lasting tonic- or phasic-firing pattern (Figure 17D) characteristic of inhibitory spinal cord interneurons (Cui et al., 2011). These results show that TRPV1 is functionally expressed in a substantial subpopulation of GABAergic SG neurons.

Postsynaptic Spinal TRPV1 Mediates LTD via AMPA Internalization in GABAergic SG Neurons and Results in Depression of Inhibitory Input to Projection Neurons

I next examined the role of postsynaptic spinal TRPV1 in the spinal cord synaptic circuitry involving GAD65-positive SG neurons. Application of capsaicin induced a long-lasting depression of EPSCs evoked in SG neurons by electrical stimulation of the dorsal root entry zone (DREZ). This effect of capsaicin was abolished in slices prepared from TRPV1$^{-/-}$ mice and also when intracellular 6-iodo-capsaicin was introduced by the patch pipette (Figure 18A). Consistent with a postsynaptic action of capsaicin in LTD, the inclusion of 6-iodo-capsaicin in the patch pipette did not inhibit spontaneous EPSCs induced by presynaptic-TRPV1 activation (Figure 19A). The capsaicin-induced LTD persisted in RTX-treated mice (Figure 18B) and capsaicin did not affect the

paired-pulse ratio (Figure 18C), suggesting that the LTD is independent of TRPV1-expressing afferents and is not mediated by changes in presynaptic neurotransmitter release. Capsaicin-induced LTD was not observed when intracellular calcium was buffered by 1,2-bis(o-aminophenoxy)ethane-N,N,N',N'-tetraacetic acid (BAPTA) in the recording pipette (Figure 18B) confirming that elevation of postsynaptic of calcium is required for synaptic depression by capsaicin. The capsaicin-induced LTD of EPSC was not dependent on the activity of NMDA receptors, group I and II metabotropic glutamate receptors (mGluR), or the substance P receptor neurokinin 1 as the effect was not blocked by application of the antagonists AP5 (50 µM), Hexyl-HIBO (HIBO, Group I mGluR antagonist, 200 µM), LY341495 (Group II mGluR antagonist, 100 µM) (Figure 18B), (RS)-α-methyl-4-carboxyphenylglycine (MCPG, non-selective group I/group II mGluR antagonist, 500 µM) and L-703,606 (10 µM) (Figure 19B), respectively. Thus I tested the involvement of alpha-amino-3-hydroxy-5-methyl-4-isoxazolepropionic acid (AMPA) receptors as a likely candidate mediating TRPV1-dependent synaptic inhibition. I observed that whole-cell currents elicited by focal application of AMPA were reduced after capsaicin application (68.08 ± 3.39%, Figure 18D); the reduction in AMPA current was not observed in the presence of 6-iodo-capsaicin (Figure 19C and 19D). This finding was consistent with a postsynaptic locus and suggested altered membrane expression of AMPA receptors. Indeed, following capsaicin application to spinal cord slices I observed a reduction in membrane expression of AMPA receptor subunit GluA2 (GluR2) protein (60.4 ± 9.8%), the main AMPA subunit in the SG (Polgar et al., 2008) (Figure 18E).

To examine the functional consequences of capsaicin-induced LTD in

GABAergic SG interneurons I retrogradely labeled spinothalamic tract (STT) projection neurons by injection of 1,1',di-octadecyl-3,3,3'3'-tetramethylindocarbocyanine perchlorate (DiI) into the ventroposterolateral (VPL) subnucleus of the thalamus (Figure 18F). Labeled neurons were located in the deep lamina of the spinal dorsal horn and showed inhibitory postsynaptic currents (IPSCs) in response to DREZ stimulation (Figure 18F and Figure 20) that were blocked by CNQX (10 μM) and AP5 (50 μM), confirming their polysynaptic nature. The amplitude of DREZ-evoked IPSCs in STT neurons from wild-type (Wt) and RTX-treated mice was decreased after capsaicin application, and depression of IPSCs (Wt, 56 ± 11%; RTX-treated mice, 65 ± 9%) lasted for at least 15 min (Figure 18F). The reduction in IPSC amplitude was not the result of a direct action of capsaicin on STT neurons as TRPV1 mRNA was not detected in STT neurons by single-cell RT-PCR (Figure 18F). Together, these data suggest that activation of TRPV1 leads to depression of excitatory input to GABAergic SG interneurons by a postsynaptic mechanism involving intracellular calcium-dependent GluA2 (GluR2) internalization, thus resulting in reduced inhibitory input to STT neurons (Figure 18G).

Postsynaptic Spinal TRPV1 Is Involved in the Maintenance of Chronic Mechanical Allodynia after Nerve Injury

To determine whether activation of spinal TRPV1 plays a role in the development of neuropathic pain, I measured mechanical sensitivity in a chronic constriction injury (CCI) model. Accumulating mechanical hypersensitivity up to 28 days after CCI was attenuated by ~41% in TRPV1-/- mice (Figure 21A and 21C) but not in RTX-treated mice (Figure 21B and 21C).

Furthermore, spinal TRPV1 inhibition by intrathecal administration of BCTC dose-dependently alleviated chronic mechanical pain in RTX-treated mice following CCI (Figure 21D and 21E). By restricting TRPV1 blockade to the spinal cord CNS using intrathecal injection, we were able to avoid the induction of hyperthermia that occurred with systemic (intravenous) administration of BCTC (Figure 21F).

Figure 14. Spinal TRPV1 in central neurons mediates mechanical allodynia

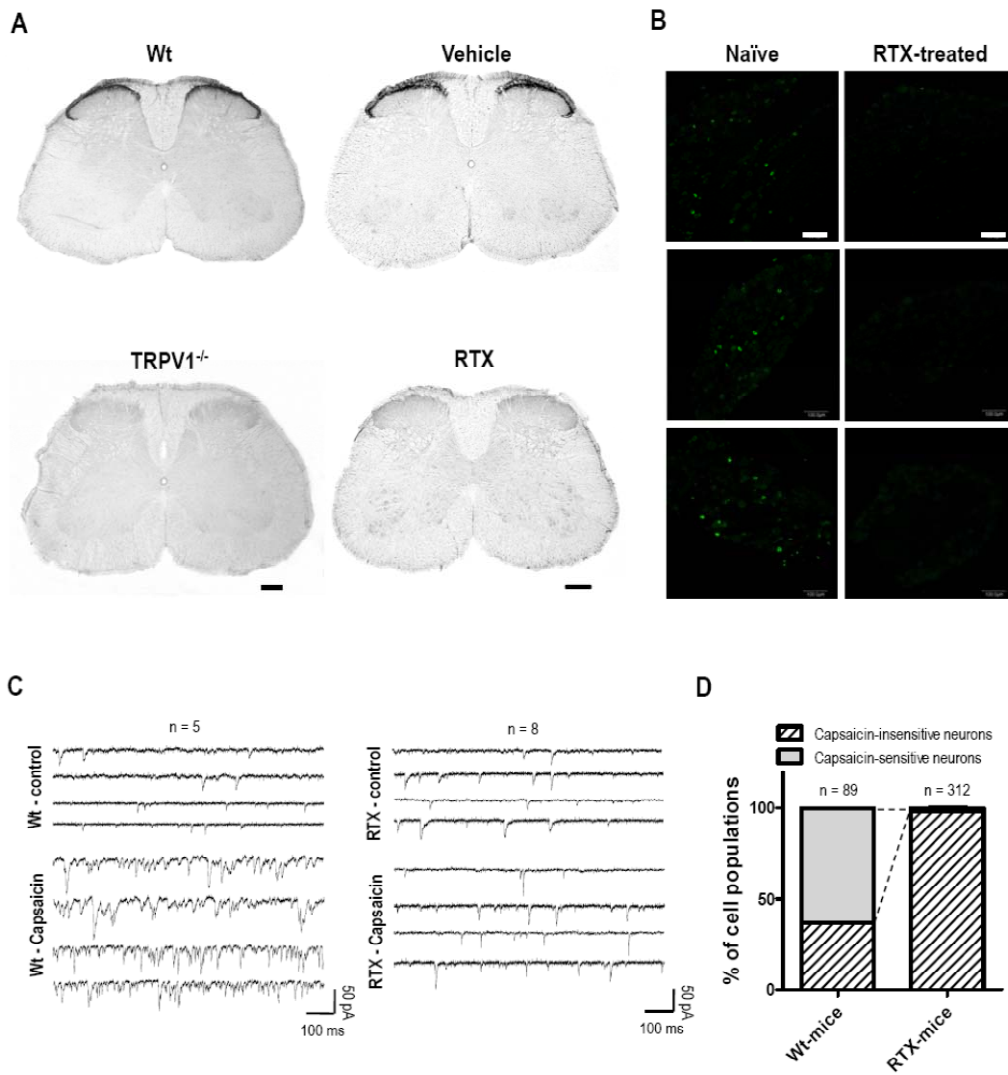(A, B) Mechanical thresholds were measured after intrathecal administration of capsaicin. (A) Time course after injection of capsaicin (1 μg, n = 6), capsaicin (1 μg) with BCTC (10 μg, n =6) and vehicle with BCTC alone (10 μg, n = 5) in naïve mice. (B) Time course after injection of capsaicin (1 μg) in TRPV1$^{-/-}$(n = 5) and RTX-treated mice (n = 6). One-way repeated measures ANOVA of changes in mechanical threshold by capsaicin, *$P<0.05$, **$P<0.005$. (C) Expression level of TRPV1 mRNA was markedly decreased in dorsal root ganglion but not in spinal cord (n = 3, unpaired t-test; **$P<0.001$) 7 days after intraperitoneal injection of RTX. (D-G) Electron microscopic immunostaining for TRPV1 in the superficial lamina of the spinal dorsal horn in naïve (D-F) and TRPV1$^{-/-}$ mice (G). (D) TRPV1 immunostaining is observed in an axon terminal containing spherical vesicles that is presynaptic to a dendrite, (E) in a dendrite that is postsynaptic to an axon terminal and (F) within somata (*inset;* higher magnification of boxed area). (G) TRPV1 immunostaining is completely abolished in the spinal dorsal horn of the TRPV1$^{-/-}$ mice. Arrow indicates TRPV1 immunoreaction product. At, axon terminal; d, dendrite. Scale bar, 200 nm in D, E, F-*inset* and G and 1 μm in F.

A

B

C

D

E

F

G
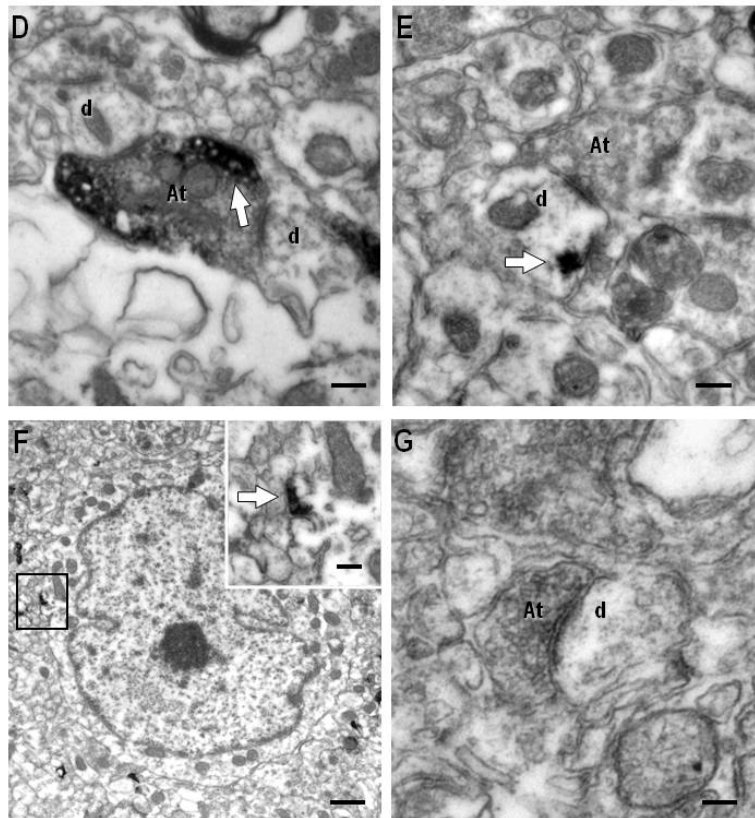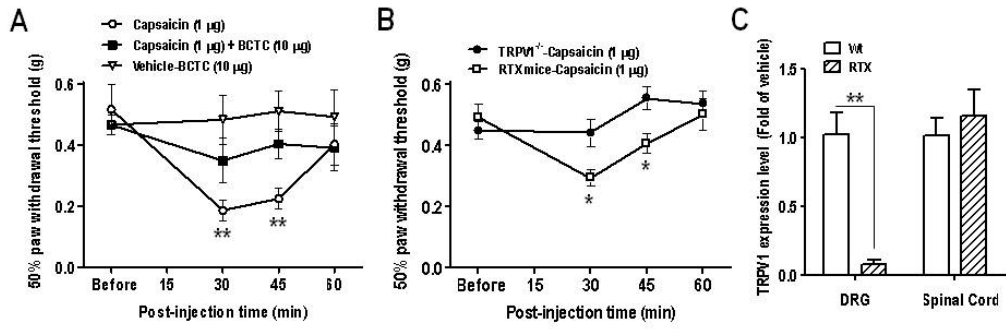
Figure 15. Expression of TRPV1 in the spinal cord and DRG of adult mice

(A) Photomicrographs showing immunoreactivity for TRPV1 in the spinal dorsal horn of wild-type (*upper left*), TRPV1$^{-/-}$ (*lower left*), vehicle-treated (*upper right*) and RTX-treated mice (*lower right*). TRPV1 immunostaining is observed in the superficial lamina of the spinal dorsal horn of the wild-type and vehicle-treated mice, while immunostaining is absent from the dorsal horn of the TRPV1$^{-/-}$ and RTX-treated mice. Scale bar, 200 μm. (B) Photomicrographs showing immunoreactivity for TRPV1 in the dorsal root ganglion (DRG) of naïve (*left*) and RTX-treated mice (*right*). (C) Application of capsaicin (2 μM) increased the frequency of spontaneous EPSCs in SG neurons from wild-type (Wt, *left*) mice, but not from RTX-treated mice (*right)*. (E) Histogram showing percentage of DRG neurons responding to capsaicin with $[Ca^{2+}]_i$ transients in Wt and RTX-treated mice. Neurons were confirmed by their response to high potassium solution.

A

Wt

Vehicle

TRPV1⁻/⁻

RTX

B

Naïve   RTX-treated

C

n = 5

Wt - control

Wt - Capsaicin

n = 8

RTX - control

RTX - Capsaicin

50 pA

100 ms

50 pA

100 ms

D

Capsaicin-insensitive neurons
Capsaicin-sensitive neurons

n = 89   n = 312

% of cell populations

Wt-mice   RTX-mice

Figure 16. TRPV1 is functionally expressed by GAD-positive SG neurons

(A) Electron micrograph of immunoperoxidase staining for TRPV1 combined with immunogold labeling for glutamic acid decarboxylase (GAD) in spinal dorsal horn of mice. TRPV1 (arrow) and GAD (arrow head) were detected in the same dendrites. Scale bar, 500 nm. (B), Single-cell RT-PCR revealed that TRPV1 mRNA was expressed predominantly in a population of GAD65-EGFP positive SG neurons (n = 23/30) but in also in a small population of GAD65-EGFP negative SG neurons (n = 5/20, ***P=0.0005, Fisher's exact test). (C, D) Functional expression of TRPV1 in GAD65-EGFP positive SG neurons. (C) Capsaicin (CAP, 2 μM)-induced currents were blocked by 50 μM 6-iodonordihydrocapsaicin (6-iodo-CAP, n = 6, *P=3.61e-8). (D) I–V relationship (-90 to +40 mV) obtained from capsaicin-induced currents.

A

B

cell1 cell2 cell3 cell4 cell5 PC

GAD65+

TRPV1

β-actin

TRPV1−
(n = 7)

TRPV1+
(n = 23) ***

GAD65−

TRPV1

β-actin

TRPV1−
(n = 15)

TRPV1+
(n = 5)

C

50 μM 6-iodo-CAP

CAP   CAP   CAP

20 pA
10 s

Normalized response
(% of 1st CAP)

Control   6-Iodo-CAP   Washout

*

D

CAP

10 pA
30 s

I (pA)

V (mV)

-100   -80   -40   0   40

100

50

-50

-100
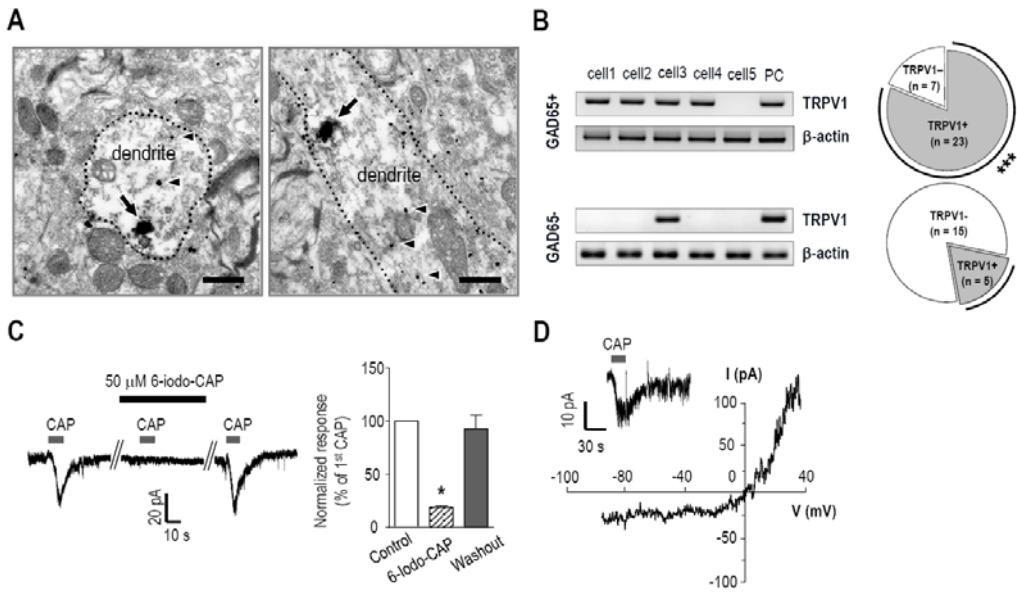
Figure 17. Functional expression of TRPV1 in tonic- and phasic-firing postsynaptic SG neurons

(A-C) Capsaicin (2 μM, CAP)-induced inward currents were elicited at -70mV of holding potential in normal aCSF (A) and in modified aCSF with a cocktail of neurotransmission blockers (B). I-V relationship (-90 mV to +40mV, 500 ms) obtained from CAP-induced currents (C). I-V relationship indicated that CAP-induced currents have the characteristics of TRPV1-mediated currents with a reversal potential of ~0 mV and slight outward rectification. (D) Patterns of action potential discharge were determined by 200 pA currents injection for 2 s into GAD65-GFP SG neurons that showed CAP-induced inward currents. The tonic- and phasic-firing SG neurons were predominant among recorded SG neurons.

A

2 µM CAP

50 pA

30 s

B

2 µM CAP

5 pA

20 s

CAP-induce inward currents (pA)

n = 16

25
20
15
10
5
0

C

I (pA)

n = 3

60

30

-120   -80   -40   40

0   V (mV)

-30

D   **GAD65 (+) inhibitory SGN (5)**

n = 4/5

n = 1/5

20 mV

250 ms   200pA   200pA
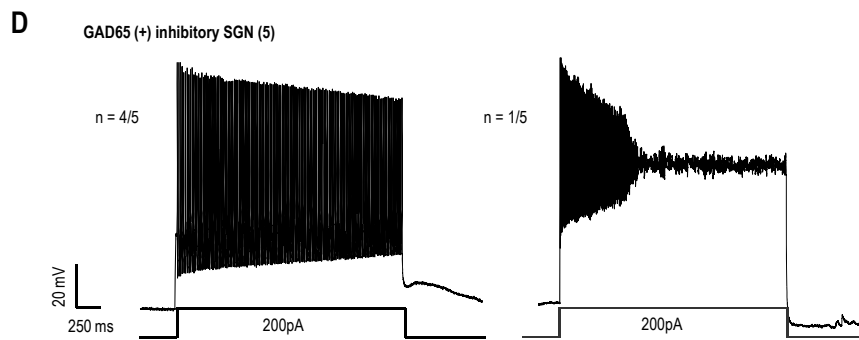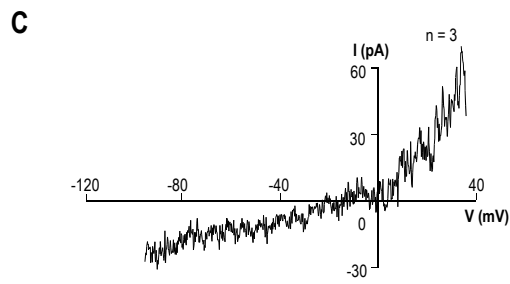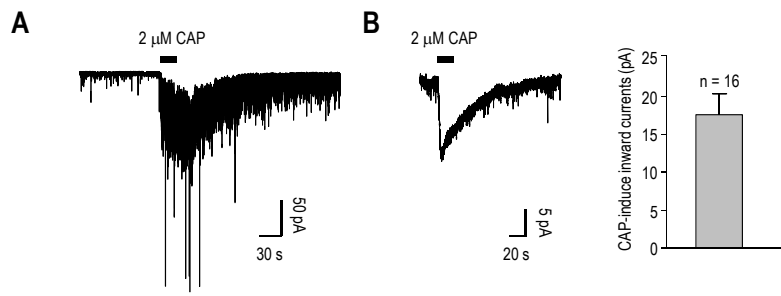
Figure 18. Capsaicin-induced LTD via reduction of membrane GluA2 (GluR2) in GAD-positive SG neurons results in depression of inhibitory input to STT neurons in spinal cord.

(A) CAP (2 μM for 5 min) induced LTD of eEPSCs (V_h = -70 mV, n = 9) in GAD65-EGFP positive SG neurons that was blocked by intra-pipette 6-iodo-CAP (50 μM, n = 5) and was absent in TRPV1$^{-/-}$ mice (n = 5). (B) CAP-induced LTD was blocked by internal administration of calcium chelator, 1,2-bis(o-aminophenoxy)ethane-N,N,N',N'-tetraacetic acid (BAPTA, 10 mM, n = 6), but not by amino-5-phosphonovaleric acid (AP5, NMDA-R blocker, 50 μM, n = 8) or Hexyl-HIBO (HIBO, Group I mGluR antagonist, 200 μM) with LY341495 (Group II mGluR antagonist, 100 μM) (n = 7). Administration of CAP consistently induced LTD in RTX-treated mice (n = 6). (C) Paired pulse ratio was obtained by a pair of stimuli given at 50 ms intervals (n = 7). (D) AMPA-induced currents were elicited by 100 μM AMPA puffing (20 - 200 ms, 3 min interval repeated puffing) at -70 mV holding potential. Bath application of capsaicin (2 μM, 5 min) decreased AMPA-induced currents (n = 6, *P=2.27e-4). (E) GluA2 receptors (GluR2) in membrane fraction was reduced by CAP (5 μM for 10 min and washout for 30 min) in lumbar spinal cord of wild-type mice, but not in TRPV1$^{-/-}$ mice (n = 3, for each group, *P=0.016). (F) Single-cell RT-PCR revealed no mRNA expression of TRPV1 in spinothalamic tract (STT) neurons. In STT neurons from both wild-type (Wt) and RTX-treated mice, evoked IPSCs at 0 mV following stimulation of dorsal root entry zone

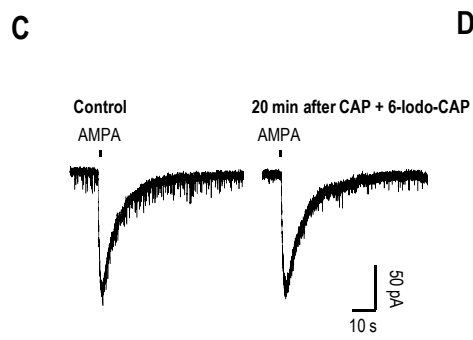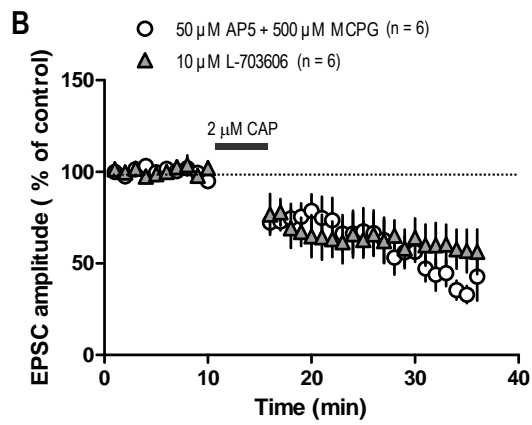(DREZ) were reduced by CAP (2 μM for 5 min and washout for 10 min, Wt; n = 6, RTX; n = 7, One-way ANOVA, Bonferroni's test; *P<0.05 (Control vs Wt-CAP or RTX-CAP group), n.s. (Wt-CAP vs RTX-CAP group). (G) Schematic representation of TRPV1 activation in GABAergic SG neurons and hypothesized sequence of events for the genesis of pain hypersensitivity through disinhibiton of nociceptive circuitry in the spinal cord.
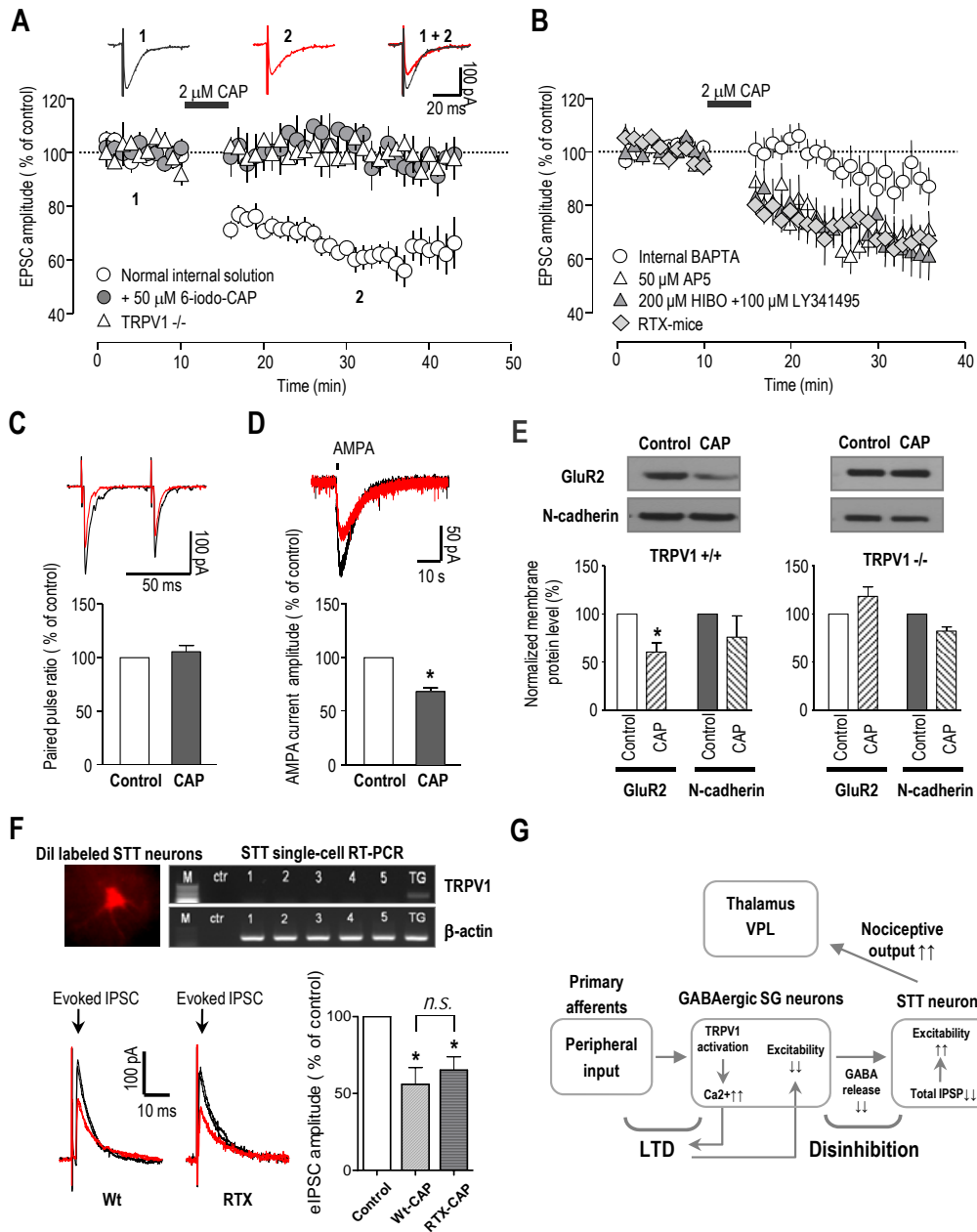
Figure 19. Activation of postsynaptic TRPV1 induces AMPA receptor internalization

(A) Application of 6-iodo-capsaicin in the patch pipette did not inhibit spontaneous EPSC induced by presynaptic activation of TRPV1. (B) CAP (2 μM for 5 min) induced LTD of eEPSCs in GAD65-EGFP positive SG neurons was not blocked by amino-5-phosphonovaleric acid (AP5, NMDA-R blocker, 50 μM) with (RS)-α-methyl-4-carboxyphenylglycine (MCPG, non-selective group I/group II mGluR antagonist, 500 μM) (n = 6) or L-703,606 (neurokinin 1 receptor antagonist, 10 μM, n = 6). (C) AMPA-induced currents were elicited by 100 μM AMPA puffing (20 - 200 ms, 3 min interval repeated puffing) at -70 mV of holding potential. Bath application of CAP did not reduce AMPA-induced currents in the presence of 50 μM 6-Iodo-CAP (97.91 ± 1.18% of control, n=5, P=0.15).

A

Internal
6-iodo-CAP

Bath
6-iodo-CAP

Control

CAP

50 pA

1 s

B

○ 50 μM AP5 + 500 μM MCPG (n = 6)
△ 10 μM L-703606 (n = 6)

2 μM CAP

EPSC amplitude (% of control)

Time (min)

C

Control

20 min after CAP + 6-Iodo-CAP

AMPA

AMPA

50 pA

10 s

D

AMPA current amplitude (% of control)

n = 5

Control   CAP +
6-Iodo-CAP
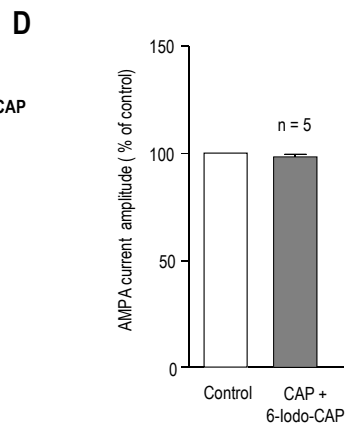
Figure 20. Inhibitory postsynaptic currents (IPSCs) are evoked by dorsal root entry zone (DREZ) stimulation in Dil-labled spinothalamic tract (STT) neurons

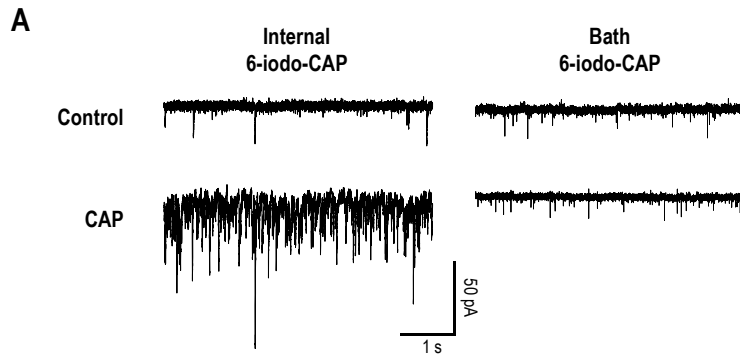(A) In Dil-labled STT neurons, evoked IPSCs at 0 mV following stimulation of DREZ were completely abolished in the presence of 5 μM picrotoxin and 2 μM strychinine, which indicate that IPSCs were not contaminated with glutamate-induced EPSCs. (B) The DREZ evoked IPSCs in STT neurons were also blocked by CNQX (10 μM) and AP5 (50 μM), suggesting that IPSCs evoked following DREZ stimulation were poly-synaptic and not a result of direct stimulation of inhibitory interneurons.
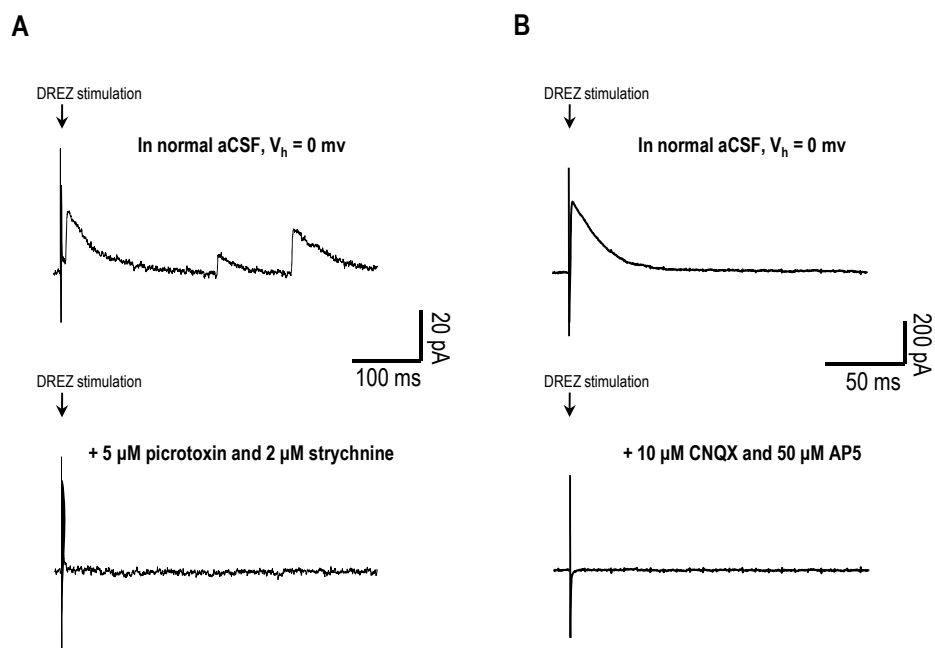
Figure 21. Chronic mechanical allodynia by nerve injury is alleviated by blockade of postsynaptic TRPV1 in spinal cord

(A, B) Changes in the mechanical thresholds after sciatic nerve chronic constriction injury (CCI) were measured in TRPV1$^{+/+}$, TRPV1$^{-/-}$, vehicle-treated and RTX-treated mice (n = 6 for each group). One-way repeated measures ANOVA followed by Bonferroni's test; **$P<0.001$ (naïve mice), #$P<0.05$, ##$P<0.001$ (TRPV1$^{-/-}$ mice vs. Presurgical value (-1 day), t-test; Ψ $P<0.05$ (naïve vs TRPV1$^{-/-}$ or vehicle-treated vs RTX-treated). (C) Mechanical hypersensitivity was calculated as the percentage difference in the mechanical thresholds of ipsilateral and contralateral hind paws accumulated from each time point up to 28 days after CCI (n = 6 for each group). One-way ANOVA followed by Bonferroni's test; *$P=0.0051$ (Wt vs TRPV1$^{-/-}$). (D) Intrathecal injection of BCTC in RTX-treated mice reversed chronic mechanical hypersensitivity at 28 days after CCI in a dose-dependent manner (n = 6 for each group). (E) The data were normalized and displayed as the maximum possible effect (MPE). Two-way ANOVA, Bonferroni's test; *$P<0.05$, **$P<0.01$. (F) Rectal body temperature measured after intravenous (i.v.) injection of BCTC (3 mg/kg) or vehicle only (50% DMSO in saline) compared with high dose intrathecal (i.t.) injection of BCTC (100 μg). (n=4 mice per group). Two-way ANOVA, Bonferroni's test; *$P<0.05$, **$P<0.01$.

A

B

C
CCI

D

E

F
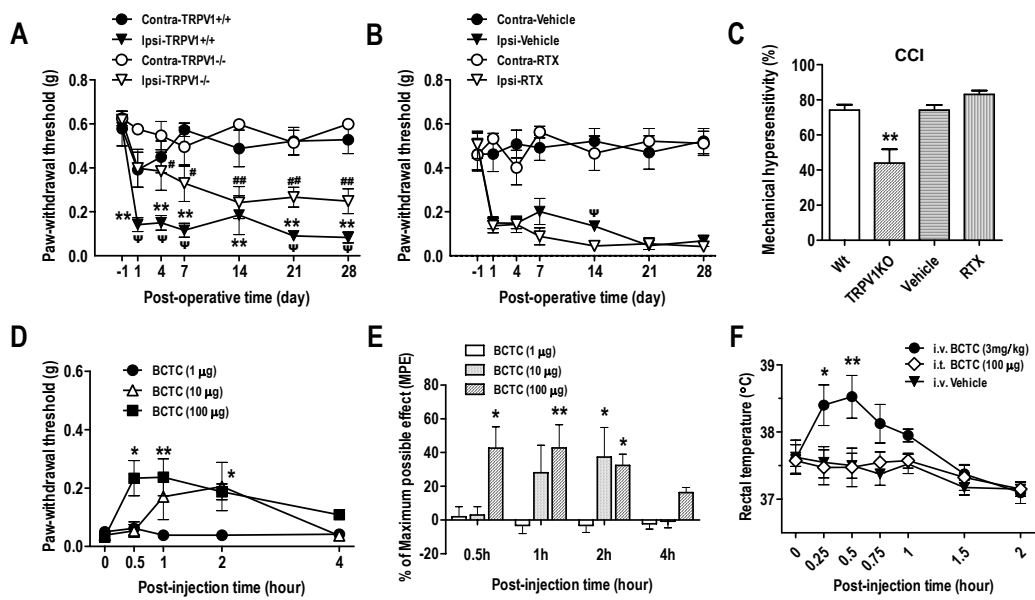
Figure 22. Spinal-TRPV1 activation by 12(S)-HPETE produces mechanical allodynia

Mechanical threshold was measured after intrathecal administration of 12(S)-HPETE (1 μg, n = 8), 12(S)-HPETE (1 μg) with BCTC (10 μg, n = 9) and BCTC alone (10 μg, n = 5) in naïve mice. One-way repeated measures ANOVA of changes in mechanical threshold by 12(S)-HPETE, *P<0.05, **P<0.005.

● 12(*S*)-HPETE (1 μg)
○ 12(*S*)-HPETE (1 μg) + BCTC (10 μg)
▼ BCTC (10 μg)
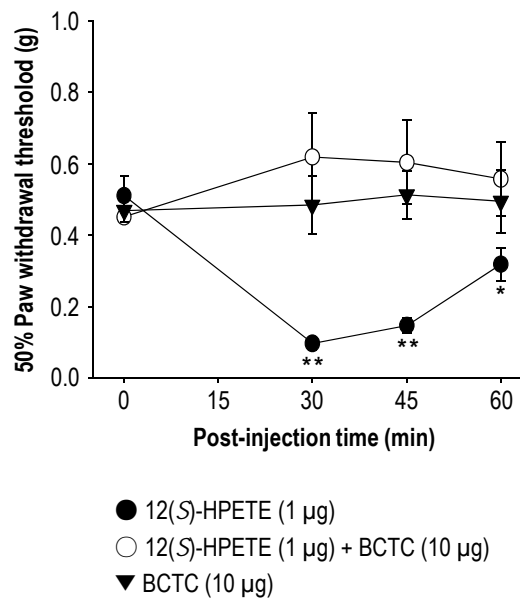
DISCUSSION

I have shown that activation of postsynaptic spinal TRPV1 leads to decreased functional AMPA receptor expression in GABAergic SG interneurons and thus reduced excitation of a key population of inhibitory interneurons. The observation of reduced inhibitory synaptic signaling to STT neurons of the deep lamina suggests a novel mechanism of 'disinhibition' of spinal cord projection neurons that are critical for the relay of nociceptive signals to higher brain centers. Using the sciatic nerve CCI model in TRPV1$^{-/-}$ mice I uncover for the first time a substantial role of TRPV1 in neuropathic mechanical pain. Furthermore, I reveal that endogenous activation of spinal TRPV1, possibly by GPCRs (Kim et al., 2009b) or arachidonic acid (AA) metabolites (Gibson et al., 2008) such as 12-hydroperoxyeicosatetraenoic acid (12-HPETE) (Figure 22) contributes to the maintenance of chronic mechanical allodynia after neuropathic nerve injury. I observed around a 40% reversal of CCI-induced mechanical allodynia by spinal application of the TRPV1 antagonist BCTC in RTX-treated mice (Figure 17D and 17E), a value comparable with a previous report on gabapentin (Pedersen et al., 2005). My observations also correlate with findings showing that TRPV1 antagonists with greater CNS penetration are more potent for reducing mechanical allodynia (Cui et al., 2006; Patapoutian et al., 2009). Finally, I have shown that by targeting spinally-mediated chronic pain we can avoid the side effects of peripheral TRPV1 blockade on temperature homeostasis (Steiner et al., 2007).

Our results help to clarify prior controversy surrounding the role of TRPV1 by explaining how it is that TRPV1 antagonists can reduce neuropathic

mechanical pain (Cui et al., 2006; Patapoutian et al., 2009) even though TRPV1-expressing primary sensory neurons do not convey physiological mechanical pain (Cavanaugh et al., 2009). A recent study using a TRPV1 reporter mouse showed that there are very few cells in the CNS that express TRPV1 (Cavanaugh et al., 2011); the results using both immuno EM and electrophysiology show that a subpopulation of interneurons in the substantia gelatinosa are among these. The TRPV1-mediated currents in these SG neurons were small (~17 pA on average), corresponding to activation of only a few dozen TRPV1 channels. Nevertheless, I find that this sparse expression of postsynaptic TRPV1 channels in a key population of neurons has major functional consequences, playing a critical role in mediating mechanical allodynia.

Together with TRPV1-mediated synaptic plasticity recently demonstrated in hippocampus (Gibson et al., 2008), dentate gyrus (Chavez et al., 2010) and nucleus accumbens (Grueter et al., 2010) this work provides further evidence for the functional significance and physiological implications of TRPV1 in the CNS. In particular, the present study demonstrates that TRPV1 expression in a key population of spinal cord neurons underlies a critical role as modulator of pain transmission in spinal circuits distinct from its well-known role as a molecular transducer of pain in primary sensory neurons.

REFERENCE

Abrahamsen B, Zhao J, Asante CO, Cendan CM, Marsh S, Martinez-Barbera JP, Nassar MA, Dickenson AH, Wood JN (2008) The cell and molecular basis of mechanical, cold, and inflammatory pain. Science 321:702-705.

Alvarez FJ, Villalba RM, Carr PA, Grandes P, Somohano PM (2000) Differential distribution of metabotropic glutamate receptors 1a, 1b, and 5 in the rat spinal cord. J Comp Neurol 422:464-487.

Bae YC, Oh JM, Hwang SJ, Shigenaga Y, Valtschanoff JG (2004) Expression of vanilloid receptor TRPV1 in the rat trigeminal sensory nuclei. J Comp Neurol 478:62-71.

Basbaum AI, Bautista DM, Scherrer G, Julius D (2009) Cellular and molecular mechanisms of pain. Cell 139:267-284.

Bevan S, Szolcsanyi J (1990) Sensory neuron-specific actions of capsaicin: mechanisms and applications. Trends Pharmacol Sci 11:330-333.

Bhave G, Karim F, Carlton SM, Gereau RWt (2001) Peripheral group I metabotropic glutamate receptors modulate nociception in mice. Nat Neurosci 4:417-423.

Bhave G, Zhu W, Wang H, Brasier DJ, Oxford GS, Gereau RWt (2002) cAMP-dependent protein kinase regulates desensitization of the capsaicin receptor (VR1) by direct phosphorylation. Neuron 35:721-731.

Bhave G, Hu HJ, Glauner KS, Zhu W, Wang H, Brasier DJ, Oxford GS, Gereau RWt (2003) Protein kinase C phosphorylation sensitizes but does not activate the capsaicin receptor transient receptor potential vanilloid 1

(TRPV1). Proc Natl Acad Sci U S A 100:12480-12485.

Bolcskei K, Helyes Z, Szabo A, Sandor K, Elekes K, Nemeth J, Almasi R, Pinter E, Petho G, Szolcsanyi J (2005) Investigation of the role of TRPV1 receptors in acute and chronic nociceptive processes using gene-deficient mice. Pain 117:368-376.

Campbell JN, Meyer RA (2006) Mechanisms of neuropathic pain. Neuron 52:77-92.

Caterina MJ, Julius D (2001) The vanilloid receptor: a molecular gateway to the pain pathway. Annu Rev Neurosci 24:487-517.

Caterina MJ, Rosen TA, Tominaga M, Brake AJ, Julius D (1999) A capsaicin-receptor homologue with a high threshold for noxious heat. Nature 398:436-441.

Caterina MJ, Schumacher MA, Tominaga M, Rosen TA, Levine JD, Julius D (1997) The capsaicin receptor: a heat-activated ion channel in the pain pathway. Nature 389:816-824.

Caterina MJ, Leffler A, Malmberg AB, Martin WJ, Trafton J, Petersen-Zeitz KR, Koltzenburg M, Basbaum AI, Julius D (2000) Impaired nociception and pain sensation in mice lacking the capsaicin receptor. Science 288:306-313.

Cavanaugh DJ, Lee H, Lo L, Shields SD, Zylka MJ, Basbaum AI, Anderson DJ (2009) Distinct subsets of unmyelinated primary sensory fibers mediate behavioral responses to noxious thermal and mechanical stimuli. Proc Natl Acad Sci U S A 106:9075-9080.

Cavanaugh DJ, Chesler AT, Jackson AC, Sigal YM, Yamanaka H, Grant R, O'Donnell D, Nicoll RA, Shah NM, Julius D, Basbaum AI (2011) Trpv1 reporter mice reveal highly restricted brain distribution and functional

expression in arteriolar smooth muscle cells. J Neurosci 31:5067-5077.

Chaplan SR, Bach FW, Pogrel JW, Chung JM, Yaksh TL (1994) Quantitative assessment of tactile allodynia in the rat paw. J Neurosci Methods 53:55-63.

Chavez AE, Chiu CQ, Castillo PE (2010) TRPV1 activation by endogenous anandamide triggers postsynaptic long-term depression in dentate gyrus. Nat Neurosci 13:1511-1518.

Chu CJ, Huang SM, De Petrocellis L, Bisogno T, Ewing SA, Miller JD, Zipkin RE, Daddario N, Appendino G, Di Marzo V, Walker JM (2003) N-oleoyldopamine, a novel endogenous capsaicin-like lipid that produces hyperalgesia. J Biol Chem 278:13633-13639.

Chuang HH, Prescott ED, Kong H, Shields S, Jordt SE, Basbaum AI, Chao MV, Julius D (2001) Bradykinin and nerve growth factor release the capsaicin receptor from PtdIns(4,5)P2-mediated inhibition. Nature 411:957-962.

Chung MK, Lee H, Mizuno A, Suzuki M, Caterina MJ (2004) TRPV3 and TRPV4 mediate warmth-evoked currents in primary mouse keratinocytes. J Biol Chem 279:21569-21575.

Clapham DE (2003) TRP channels as cellular sensors. Nature 426:517-524.

Correll CC, Phelps PT, Anthes JC, Umland S, Greenfeder S (2004) Cloning and pharmacological characterization of mouse TRPV1. Neurosci Lett 370:55-60.

Costigan M, Scholz J, Woolf CJ (2009) Neuropathic pain: a maladaptive response of the nervous system to damage. Annu Rev Neurosci 32:1-32.

Coull JA, Boudreau D, Bachand K, Prescott SA, Nault F, Sik A, De Koninck P, De Koninck Y (2003) Trans-synaptic shift in anion gradient in spinal

lamina I neurons as a mechanism of neuropathic pain. Nature 424:938-942.

Coull JA, Beggs S, Boudreau D, Boivin D, Tsuda M, Inoue K, Gravel C, Salter MW, De Koninck Y (2005) BDNF from microglia causes the shift in neuronal anion gradient underlying neuropathic pain. Nature 438:1017-1021.

Cui L, Kim YR, Kim HY, Lee SC, Shin HS, Szabo G, Erdelyi F, Kim J, Kim SJ (2011) Modulation of synaptic transmission from primary afferents to spinal substantia gelatinosa neurons by group III mGluRs in GAD65-EGFP transgenic mice. J Neurophysiol 105:1102-1111.

Cui M, Honore P, Zhong C, Gauvin D, Mikusa J, Hernandez G, Chandran P, Gomtsyan A, Brown B, Bayburt EK, Marsh K, Bianchi B, McDonald H, Niforatos W, Neelands TR, Moreland RB, Decker MW, Lee CH, Sullivan JP, Faltynek CR (2006) TRPV1 receptors in the CNS play a key role in broad-spectrum analgesia of TRPV1 antagonists. J Neurosci 26:9385-9393.

Davis JB, Gray J, Gunthorpe MJ, Hatcher JP, Davey PT, Overend P, Harries MH, Latcham J, Clapham C, Atkinson K, Hughes SA, Rance K, Grau E, Harper AJ, Pugh PL, Rogers DC, Bingham S, Randall A, Sheardown SA (2000) Vanilloid receptor-1 is essential for inflammatory thermal hyperalgesia. Nature 405:183-187.

De Petrocellis L, Harrison S, Bisogno T, Tognetto M, Brandi I, Smith GD, Creminon C, Davis JB, Geppetti P, Di Marzo V (2001) The vanilloid receptor (VR1)-mediated effects of anandamide are potently enhanced by the cAMP-dependent protein kinase. J Neurochem 77:1660-1663.

deGroot J, Zhou S, Carlton SM (2000) Peripheral glutamate release in the

hindpaw following low and high intensity sciatic stimulation. Neuroreport 11:497-502.

Delmas P, Wanaverbecq N, Abogadie FC, Mistry M, Brown DA (2002) Signaling microdomains define the specificity of receptor-mediated InsP(3) pathways in neurons. Neuron 34:209-220.

Di Marzo V, Blumberg PM, Szallasi A (2002) Endovanilloid signaling in pain. Curr Opin Neurobiol 12:372-379.

Dixon WJ (1980) Efficient analysis of experimental observations. Annu Rev Pharmacol Toxicol 20:441-462.

Docherty RJ, Yeats JC, Piper AS (1997) Capsazepine block of voltage-activated calcium channels in adult rat dorsal root ganglion neurones in culture. Br J Pharmacol 121:1461-1467.

Ferrer-Montiel A, Garcia-Martinez C, Morenilla-Palao C, Garcia-Sanz N, Fernandez-Carvajal A, Fernandez-Ballester G, Planells-Cases R (2004) Molecular architecture of the vanilloid receptor. Insights for drug design. Eur J Biochem 271:1820-1826.

Ferrini F, Salio C, Lossi L, Gambino G, Merighi A (2010) Modulation of inhibitory neurotransmission by the vanilloid receptor type 1 (TRPV1) in organotypically cultured mouse substantia gelatinosa neurons. Pain 150:128-140.

Finnerup NB, Sindrup SH, Jensen TS (2007) Chronic neuropathic pain: mechanisms, drug targets and measurement. Fundam Clin Pharmacol 21:129-136.

Fisher K, Coderre TJ (1998) Hyperalgesia and allodynia induced by intrathecal (RS)-dihydroxyphenylglycine in rats. Neuroreport 9:1169-1172.

Gibson HE, Edwards JG, Page RS, Van Hook MJ, Kauer JA (2008) TRPV1

channels mediate long-term depression at synapses on hippocampal interneurons. Neuron 57:746-759.

Grueter BA, Brasnjo G, Malenka RC (2010) Postsynaptic TRPV1 triggers cell type-specific long-term depression in the nucleus accumbens. Nat Neurosci 13:1519-1525.

Gunthorpe MJ, Harries MH, Prinjha RK, Davis JB, Randall A (2000) Voltage- and time-dependent properties of the recombinant rat vanilloid receptor (rVR1). J Physiol 525 Pt 3:747-759.

Guo A, Simone DA, Stone LS, Fairbanks CA, Wang J, Elde R (2001) Developmental shift of vanilloid receptor 1 (VR1) terminals into deeper regions of the superficial dorsal horn: correlation with a shift from TrkA to Ret expression by dorsal root ganglion neurons. Eur J Neurosci 14:293-304.

Hermans E, Challiss RA (2001) Structural, signalling and regulatory properties of the group I metabotropic glutamate receptors: prototypic family C G-protein-coupled receptors. Biochem J 359:465-484.

Hu HJ, Alter BJ, Carrasquillo Y, Qiu CS, Gereau RWt (2007) Metabotropic glutamate receptor 5 modulates nociceptive plasticity via extracellular signal-regulated kinase-Kv4.2 signaling in spinal cord dorsal horn neurons. J Neurosci 27:13181-13191.

Huang SM, Bisogno T, Trevisani M, Al-Hayani A, De Petrocellis L, Fezza F, Tognetto M, Petros TJ, Krey JF, Chu CJ, Miller JD, Davies SN, Geppetti P, Walker JM, Di Marzo V (2002) An endogenous capsaicin-like substance with high potency at recombinant and native vanilloid VR1 receptors. Proc Natl Acad Sci U S A 99:8400-8405.

Hwang SJ, Burette A, Rustioni A, Valtschanoff JG (2004) Vanilloid receptor

VR1-positive primary afferents are glutamatergic and contact spinal neurons that co-express neurokinin receptor NK1 and glutamate receptors. J Neurocytol 33:321-329.

Hwang SW, Cho H, Kwak J, Lee SY, Kang CJ, Jung J, Cho S, Min KH, Suh YG, Kim D, Oh U (2000) Direct activation of capsaicin receptors by products of lipoxygenases: endogenous capsaicin-like substances. Proc Natl Acad Sci U S A 97:6155-6160.

Hylden JL, Wilcox GL (1980) Intrathecal morphine in mice: a new technique. Eur J Pharmacol 67:313-316.

Ikeda H, Heinke B, Ruscheweyh R, Sandkuhler J (2003) Synaptic plasticity in spinal lamina I projection neurons that mediate hyperalgesia. Science 299:1237-1240.

Iwata H, Takasusuki T, Yamaguchi S, Hori Y (2007) NMDA receptor 2B subunit-mediated synaptic transmission in the superficial dorsal horn of peripheral nerve-injured neuropathic mice. Brain Res 1135:92-101.

Ji RR, Samad TA, Jin SX, Schmoll R, Woolf CJ (2002) p38 MAPK activation by NGF in primary sensory neurons after inflammation increases TRPV1 levels and maintains heat hyperalgesia. Neuron 36:57-68.

Jia H, Rustioni A, Valtschanoff JG (1999) Metabotropic glutamate receptors in superficial laminae of the rat dorsal horn. J Comp Neurol 410:627-642.

Jordt SE, Julius D (2002) Molecular basis for species-specific sensitivity to "hot" chili peppers. Cell 108:421-430.

Jordt SE, Tominaga M, Julius D (2000) Acid potentiation of the capsaicin receptor determined by a key extracellular site. Proc Natl Acad Sci U S A 97:8134-8139.

Julius D, Basbaum AI (2001) Molecular mechanisms of nociception. Nature

413:203-210.

Jung J, Hwang SW, Kwak J, Lee SY, Kang CJ, Kim WB, Kim D, Oh U (1999)
Capsaicin binds to the intracellular domain of the capsaicin-activated
ion channel. J Neurosci 19:529-538.

Jung SJ, Kim SJ, Park YK, Oh SB, Cho K, Kim J (2006) Group I mGluR
regulates the polarity of spike-timing dependent plasticity in substantia
gelatinosa neurons. Biochem Biophys Res Commun 347:509-516.

Kanai Y, Hara T, Imai A (2006) Participation of the spinal TRPV1 receptors in
formalin-evoked pain transduction: a study using a selective TRPV1
antagonist, iodo-resiniferatoxin. J Pharm Pharmacol 58:489-493.

Kim H, Cui L, Kim J, Kim SJ (2009a) Transient receptor potential vanilloid
type 1 receptor regulates glutamatergic synaptic inputs to the
spinothalamic tract neurons of the spinal cord deep dorsal horn.
Neuroscience 160:508-516.

Kim YH, Park CK, Back SK, Lee CJ, Hwang SJ, Bae YC, Na HS, Kim JS, Jung
SJ, Oh SB (2009b) Membrane-delimited coupling of TRPV1 and
mGluR5 on presynaptic terminals of nociceptive neurons. J Neurosci
29:10000-10009.

Kuner R (2010) Central mechanisms of pathological pain. Nat Med 16:1258-
1266.

Kwak J, Wang MH, Hwang SW, Kim TY, Lee SY, Oh U (2000) Intracellular
ATP increases capsaicin-activated channel activity by interacting with
nucleotide-binding domains. J Neurosci 20:8298-8304.

Lesage ASJ (2004) Role of group I metabotropic glutamate receptors mGlu1
and mGlu5 in nociceptive signalling. Current Neuropharmacology
2:363–393

Livak KJ, Schmittgen TD (2001) Analysis of relative gene expression data using real-time quantitative PCR and the 2(-Delta Delta C(T)) Method. Methods 25:402-408.

Lopez-Bendito G, Sturgess K, Erdelyi F, Szabo G, Molnar Z, Paulsen O (2004) Preferential origin and layer destination of GAD65-GFP cortical interneurons. Cereb Cortex 14:1122-1133.

Lu Y, Perl ER (2005) Modular organization of excitatory circuits between neurons of the spinal superficial dorsal horn (laminae I and II). J Neurosci 25:3900-3907.

Marvizon JC, Wang X, Matsuka Y, Neubert JK, Spigelman I (2003) Relationship between capsaicin-evoked substance P release and neurokinin 1 receptor internalization in the rat spinal cord. Neuroscience 118:535-545.

Maxwell DJ, Belle MD, Cheunsuang O, Stewart A, Morris R (2007) Morphology of inhibitory and excitatory interneurons in superficial laminae of the rat dorsal horn. J Physiol 584:521-533.

Melzack R, Wall PD (1965) Pain mechanisms: a new theory. Science 150:971-979.

Michael GJ, Priestley JV (1999) Differential expression of the mRNA for the vanilloid receptor subtype 1 in cells of the adult rat dorsal root and nodose ganglia and its downregulation by axotomy. J Neurosci 19:1844-1854.

Mohapatra DP, Nau C (2003) Desensitization of capsaicin-activated currents in the vanilloid receptor TRPV1 is decreased by the cyclic AMP-dependent protein kinase pathway. J Biol Chem 278:50080-50090.

Moore KA, Kohno T, Karchewski LA, Scholz J, Baba H, Woolf CJ (2002) Partial peripheral nerve injury promotes a selective loss of GABAergic inhibition in the superficial dorsal horn of the spinal cord. J Neurosci 22:6724-6731.

Morenilla-Palao C, Planells-Cases R, Garcia-Sanz N, Ferrer-Montiel A (2004) Regulated exocytosis contributes to protein kinase C potentiation of vanilloid receptor activity. J Biol Chem 279:25665-25672.

Moriyama T, Higashi T, Togashi K, Iida T, Segi E, Sugimoto Y, Tominaga T, Narumiya S, Tominaga M (2005) Sensitization of TRPV1 by EP1 and IP reveals peripheral nociceptive mechanism of prostaglandins. Mol Pain 1:3.

Moriyama T, Iida T, Kobayashi K, Higashi T, Fukuoka T, Tsumura H, Leon C, Suzuki N, Inoue K, Gachet C, Noguchi K, Tominaga M (2003) Possible involvement of P2Y2 metabotropic receptors in ATP-induced transient receptor potential vanilloid receptor 1-mediated thermal hypersensitivity. J Neurosci 23:6058-6062.

Numazaki M, Tominaga T, Toyooka H, Tominaga M (2002) Direct phosphorylation of capsaicin receptor VR1 by protein kinase Cepsilon and identification of two target serine residues. J Biol Chem 277:13375-13378.

Oh SB, Tran PB, Gillard SE, Hurley RW, Hammond DL, Miller RJ (2001) Chemokines and glycoprotein120 produce pain hypersensitivity by directly exciting primary nociceptive neurons. J Neurosci 21:5027-5035.

Oh U, Hwang SW, Kim D (1996) Capsaicin activates a nonselective cation channel in cultured neonatal rat dorsal root ganglion neurons. J Neurosci 16:1659-1667.

Ohta T, Komatsu R, Imagawa T, Otsuguro K, Ito S (2005) Molecular cloning, functional characterization of the porcine transient receptor potential V1 (pTRPV1) and pharmacological comparison with endogenous pTRPV1. Biochem Pharmacol 71:173-187.

Oliet SH, Piet R, Poulain DA (2001) Control of glutamate clearance and synaptic efficacy by glial coverage of neurons. Science 292:923-926.

Park CK, Kim MS, Fang Z, Li HY, Jung SJ, Choi SY, Lee SJ, Park K, Kim JS, Oh SB (2006) Functional expression of thermo-transient receptor potential channels in dental primary afferent neurons: implication for tooth pain. J Biol Chem 281:17304-17311.

Patapoutian A, Tate S, Woolf CJ (2009) Transient receptor potential channels: targeting pain at the source. Nat Rev Drug Discov 8:55-68.

Patwardhan AM, Scotland PE, Akopian AN, Hargreaves KM (2009) Activation of TRPV1 in the spinal cord by oxidized linoleic acid metabolites contributes to inflammatory hyperalgesia. Proc Natl Acad Sci U S A 106:18820-18824.

Pedersen LH, Nielsen AN, Blackburn-Munro G (2005) Anti-nociception is selectively enhanced by parallel inhibition of multiple subtypes of monoamine transporters in rat models of persistent and neuropathic pain. Psychopharmacology (Berl) 182:551-561.

Peier AM, Moqrich A, Hergarden AC, Reeve AJ, Andersson DA, Story GM, Earley TJ, Dragoni I, McIntyre P, Bevan S, Patapoutian A (2002a) A TRP channel that senses cold stimuli and menthol. Cell 108:705-715.

Peier AM, Reeve AJ, Andersson DA, Moqrich A, Earley TJ, Hergarden AC, Story GM, Colley S, Hogenesch JB, McIntyre P, Bevan S, Patapoutian A (2002b) A heat-sensitive TRP channel expressed in keratinocytes.

Science 296:2046-2049.

Phillips E, Reeve A, Bevan S, McIntyre P (2004) Identification of species-specific determinants of the action of the antagonist capsazepine and the agonist PPAHV on TRPV1. J Biol Chem 279:17165-17172.

Piper AS, Yeats JC, Bevan S, Docherty RJ (1999) A study of the voltage dependence of capsaicin-activated membrane currents in rat sensory neurones before and after acute desensitization. J Physiol 518 (Pt 3):721-733.

Pitcher MH, Ribeiro-Da-Silva A, Coderre TJ (2007) Effects of inflammation on the ultrastructural localization of spinal cord dorsal horn group I metabotropic glutamate receptors. J Comp Neurol 505:412-423.

Polgar E, Watanabe M, Hartmann B, Grant SG, Todd AJ (2008) Expression of AMPA receptor subunits at synapses in laminae I-III of the rodent spinal dorsal horn. Mol Pain 4:5.

Premkumar LS, Ahern GP (2000) Induction of vanilloid receptor channel activity by protein kinase C. Nature 408:985-990.

Prescott ED, Julius D (2003) A modular PIP2 binding site as a determinant of capsaicin receptor sensitivity. Science 300:1284-1288.

Puntambekar P, Mukherjea D, Jajoo S, Ramkumar V (2005) Essential role of Rac1/NADPH oxidase in nerve growth factor induction of TRPV1 expression. J Neurochem 95:1689-1703.

Ralevic V, Kendall DA, Jerman JC, Middlemiss DN, Smart D (2001) Cannabinoid activation of recombinant and endogenous vanilloid receptors. Eur J Pharmacol 424:211-219.

Rathee PK, Distler C, Obreja O, Neuhuber W, Wang GK, Wang SY, Nau C, Kress M (2002) PKA/AKAP/VR-1 module: A common link of Gs-

mediated signaling to thermal hyperalgesia. J Neurosci 22:4740-4745.

Ruegg UT, Burgess GM (1989) Staurosporine, K-252 and UCN-01: potent but nonspecific inhibitors of protein kinases. Trends Pharmacol Sci 10:218-220.

Scholz J, Woolf CJ (2002) Can we conquer pain? Nat Neurosci 5:1062-1067.

Scholz J, Broom DC, Youn DH, Mills CD, Kohno T, Suter MR, Moore KA, Decosterd I, Coggeshall RE, Woolf CJ (2005) Blocking caspase activity prevents transsynaptic neuronal apoptosis and the loss of inhibition in lamina II of the dorsal horn after peripheral nerve injury. J Neurosci 25:7317-7323.

Shin J, Cho H, Hwang SW, Jung J, Shin CY, Lee SY, Kim SH, Lee MG, Choi YH, Kim J, Haber NA, Reichling DB, Khasar S, Levine JD, Oh U (2002) Bradykinin-12-lipoxygenase-VR1 signaling pathway for inflammatory hyperalgesia. Proc Natl Acad Sci U S A 99:10150-10155.

Sikand P, Premkumar LS (2007) Potentiation of glutamatergic synaptic transmission by protein kinase C-mediated sensitization of TRPV1 at the first sensory synapse. J Physiol 581:631-647.

Sivilotti L, Woolf CJ (1994) The contribution of GABAA and glycine receptors to central sensitization: disinhibition and touch-evoked allodynia in the spinal cord. J Neurophysiol 72:169-179.

Steiner AA, Turek VF, Almeida MC, Burmeister JJ, Oliveira DL, Roberts JL, Bannon AW, Norman MH, Louis JC, Treanor JJ, Gavva NR, Romanovsky AA (2007) Nonthermal activation of transient receptor potential vanilloid-1 channels in abdominal viscera tonically inhibits autonomic cold-defense effectors. J Neurosci 27:7459-7468.

Story GM, Peier AM, Reeve AJ, Eid SR, Mosbacher J, Hricik TR, Earley TJ,

Hergarden AC, Andersson DA, Hwang SW, McIntyre P, Jegla T, Bevan S, Patapoutian A (2003) ANKTM1, a TRP-like channel expressed in nociceptive neurons, is activated by cold temperatures. Cell 112:819-829.

Sugiura T, Tominaga M, Katsuya H, Mizumura K (2002) Bradykinin lowers the threshold temperature for heat activation of vanilloid receptor 1. J Neurophysiol 88:544-548.

Sugiura Y, Lee CL, Perl ER (1986) Central projections of identified, unmyelinated (C) afferent fibers innervating mammalian skin. Science 234:358-361.

Sutton KG, Garrett EM, Rutter AR, Bonnert TP, Jarolimek W, Seabrook GR (2005) Functional characterisation of the S512Y mutant vanilloid human TRPV1 receptor. Br J Pharmacol 146:702-711.

Szallasi A, Blumberg PM (1999) Vanilloid (Capsaicin) receptors and mechanisms. Pharmacol Rev 51:159-212.

Szallasi A, Cortright DN, Blum CA, Eid SR (2007) The vanilloid receptor TRPV1: 10 years from channel cloning to antagonist proof-of-concept. Nat Rev Drug Discov 6:357-372.

Todd AJ, McKenzie J (1989) GABA-immunoreactive neurons in the dorsal horn of the rat spinal cord. Neuroscience 31:799-806.

Todd AJ, Sullivan AC (1990) Light microscope study of the coexistence of GABA-like and glycine-like immunoreactivities in the spinal cord of the rat. J Comp Neurol 296:496-505.

Todd AJ, Spike RC (1993) The localization of classical transmitters and neuropeptides within neurons in laminae I-III of the mammalian spinal dorsal horn. Prog Neurobiol 41:609-645.

Tominaga M, Caterina MJ, Malmberg AB, Rosen TA, Gilbert H, Skinner K, Raumann BE, Basbaum AI, Julius D (1998) The cloned capsaicin receptor integrates multiple pain-producing stimuli. Neuron 21:531-543.

Torsney C, MacDermott AB (2006) Disinhibition opens the gate to pathological pain signaling in superficial neurokinin 1 receptor-expressing neurons in rat spinal cord. J Neurosci 26:1833-1843.

Trevisani M, Smart D, Gunthorpe MJ, Tognetto M, Barbieri M, Campi B, Amadesi S, Gray J, Jerman JC, Brough SJ, Owen D, Smith GD, Randall AD, Harrison S, Bianchi A, Davis JB, Geppetti P (2002) Ethanol elicits and potentiates nociceptor responses via the vanilloid receptor-1. Nat Neurosci 5:546-551.

Ultenius C, Linderoth B, Meyerson BA, Wallin J (2006) Spinal NMDA receptor phosphorylation correlates with the presence of neuropathic signs following peripheral nerve injury in the rat. Neurosci Lett 399:85-90.

Urban L, Dray A (1993) Actions of capsaicin on mouse dorsal root ganglion cells in vitro. Neurosci Lett 157:187-190.

Valtschanoff JG, Rustioni A, Guo A, Hwang SJ (2001) Vanilloid receptor VR1 is both presynaptic and postsynaptic in the superficial laminae of the rat dorsal horn. J Comp Neurol 436:225-235.

van der Stelt M, Trevisani M, Vellani V, De Petrocellis L, Schiano Moriello A, Campi B, McNaughton P, Geppetti P, Di Marzo V (2005) Anandamide acts as an intracellular messenger amplifying Ca^{2+} influx via TRPV1 channels. EMBO J 24:3026-3037.

Vlachova V, Teisinger J, Susankova K, Lyfenko A, Ettrich R, Vyklicky L (2003) Functional role of C-terminal cytoplasmic tail of rat vanilloid receptor 1. J Neurosci 23:1340-1350.

Voets T, Droogmans G, Wissenbach U, Janssens A, Flockerzi V, Nilius B (2004) The principle of temperature-dependent gating in cold- and heat-sensitive TRP channels. Nature 430:748-754.

Walker K, Reeve A, Bowes M, Winter J, Wotherspoon G, Davis A, Schmid P, Gasparini F, Kuhn R, Urban L (2001a) mGlu5 receptors and nociceptive function II. mGlu5 receptors functionally expressed on peripheral sensory neurones mediate inflammatory hyperalgesia. Neuropharmacology 40:10-19.

Walker K, Bowes M, Panesar M, Davis A, Gentry C, Kesingland A, Gasparini F, Spooren W, Stoehr N, Pagano A, Flor PJ, Vranesic I, Lingenhoehl K, Johnson EC, Varney M, Urban L, Kuhn R (2001b) Metabotropic glutamate receptor subtype 5 (mGlu5) and nociceptive function. I. Selective blockade of mGlu5 receptors in models of acute, persistent and chronic pain. Neuropharmacology 40:1-9.

Woo DH, Jung SJ, Zhu MH, Park CK, Kim YH, Oh SB, Lee CJ (2008) Direct activation of Transient Receptor Potential Vanilloid 1(TRPV1) by Diacylglycerol (DAG). Mol Pain 4:42.

Woolf CJ, Fitzgerald M (1983) The properties of neurones recorded in the superficial dorsal horn of the rat spinal cord. J Comp Neurol 221:313-328.

Woolf CJ, Salter MW (2000) Neuronal plasticity: increasing the gain in pain. Science 288:1765-1769.

Woolf CJ, Shortland P, Coggeshall RE (1992) Peripheral nerve injury triggers central sprouting of myelinated afferents. Nature 355:75-78.

Yaksh TL (1989) Behavioral and autonomic correlates of the tactile evoked allodynia produced by spinal glycine inhibition: effects of modulatory

receptor systems and excitatory amino acid antagonists. Pain 37:111-123.

Yang BH, Piao ZG, Kim YB, Lee CH, Lee JK, Park K, Kim JS, Oh SB (2003) Activation of vanilloid receptor 1 (VR1) by eugenol. J Dent Res 82:781-785.

Yang K, Kumamoto E, Furue H, Yoshimura M (1998) Capsaicin facilitates excitatory but not inhibitory synaptic transmission in substantia gelatinosa of the rat spinal cord. Neurosci Lett 255:135-138.

Yasaka T, Kato G, Furue H, Rashid MH, Sonohata M, Tamae A, Murata Y, Masuko S, Yoshimura M (2007) Cell-type-specific excitatory and inhibitory circuits involving primary afferents in the substantia gelatinosa of the rat spinal dorsal horn in vitro. J Physiol 581:603-618.

Yoshimura M, Jessell TM (1989) Primary afferent-evoked synaptic responses and slow potential generation in rat substantia gelatinosa neurons in vitro. J Neurophysiol 62:96-108.

Zhang X, Huang J, McNaughton PA (2005) NGF rapidly increases membrane expression of TRPV1 heat-gated ion channels. Embo J 24:4211-4223.

Zhou HY, Chen SR, Chen H, Pan HL (2009) The glutamatergic nature of TRPV1-expressing neurons in the spinal dorsal horn. J Neurochem 108:305-318.

Zhu CZ, Hsieh G, Ei-Kouhen O, Wilson SG, Mikusa JP, Hollingsworth PR, Chang R, Moreland RB, Brioni J, Decker MW, Honore P (2005) Role of central and peripheral mGluR5 receptors in post-operative pain in rats. Pain 114:195-202.

Zygmunt PM, Petersson J, Andersson DA, Chuang H, Sorgard M, Di Marzo V, Julius D, Hogestatt ED (1999) Vanilloid receptors on sensory nerves mediate the vasodilator action of anandamide. Nature 400:452-457.

국문초록

척수 통증과민화에서 중추
transient receptor potential vanilloid-1
수용체의 역할

　　Transient receptor potential vanilloid subtype 1 (TRPV1) 수용체는 C-섬유 일차구심성 신경세포의 중추 말단에 주로 발현되며 그 길항제는 염증성 통증과 신경병증성 통증의 완화에 영향을 준다. 말초신경말단에서 TRPV1 과 metabotropic glutamate receptor 5 (mGluR5)에 의한 통증 감작 및 그 조절 현상이 제시되었지만 척수 신경으로 유입되는 감각 신경세포의 중추말단에 발현된 mGluR5와 TRPV1에 대한 기능적 발현 및 역할에 대해 아직 많이 알려져 있지 않다. 이번 연구를 통해 말초 신경의 중추 말단에서 활성화된 mGluR5에 의해 생성된 diacylglycerol (DAG)를 통한 TRPV1의 활성화 기전을 증명함으로써 mGluR5-TRPV1 의 기능적 상호작용이 병적 상황에서 중추신경과민화 형성에 중요한 역할을 하고 있음을 보여주었다.

　　또한 말초신경에 발현되어있는 TRPV1이 기계적 이질통 형성에 관여하지 않는 것으로 알려져 있지만 실제로 TRPV1의 길항제를 투여시 열 통각과민화뿐 아니라 기계적 이질통이 완화됨이 보고되었다. 이는

중추 신경에 발현되어 있는 TRPV1이 병적인 기계적 이질통 형성에 관여할 수 있음을 시사한다. 하지만 병적 상황에서 중추신경세포에 발현된 TRPV1의 역할 및 작용 기전은 거의 밝혀지지 않았다. 이러한 이유로 본 연구자는 척수신경세포에 발현된 TRPV1 역할을 알아보았다. TRPV1은 척수 substantia gelatinosa 지역의 GABAergic 억제성 신경세포에 발현되어 있고 그 활성화로 인해 long-term depression (LTD)이 형성됨을 확인 할 수 있었다. 이러한 억제성 척수신경세포의 LTD는 척수 내 통증 전달 경로의 마지막 관문인 projection 신경세포에 억제성 신호를 감소 시킴으로써 기계적 이질통 형성에 영향을 주는 것을 증명하였다. 또한 마지막으로 신경손상에 의한 만성 기계적 이질통이 척수 내 TRPV1 길항제 투약으로 인해 억제됨을 확인함으로써 TRPV1이 중요한 시냅스 조절자로 역할을 할 뿐 아니라 중추신경 특이적 TRPV1 길항제의 사용을 통해 신경병증성 통증을 치료할 수 있는 가능성을 제시하였다.